GLOBAL OPTIMIZATION FOR THE PHASE STABILITY PROBLEM

Conor M. McDonald and Christodoulos A. Floudas*
Department of Chemical Engineering
Princeton University
Princeton, N.J. 08544-5263

Submitted May 18, 1994; revised August 22, 1994; accepted by *AIChE. J.*

Abstract

The Gibbs tangent plane criterion has become an important tool in determining the quality of obtained solutions to the phase and chemical equilibrium problem. The ability to determine if a postulated solution is thermodynamically stable with respect to perturbations in any or all of the phases is very useful in the search for the true equilibrium solution. Previous approaches have concentrated on finding the stationary points of the tangent plane distance function. However, no guarantee of obtaining all stationary points can be provided. These difficulties arise due to the complex and nonlinear nature of the models used to predict equilibrium. In this work, simpler formulations for the stability problem are presented for the special class of problems where nonideal liquid phases can be adequately modeled using the NRTL and UNIQUAC activity coefficient equations. It is shown how the *global* minimum of the tangent plane distance function can be obtained for this class of problems. The advantage of a global optimization approach is that if a nonnegative solution is found, then it can be definitively asserted that the postulated solution is the globally stable equilibrium one, unlike available local algorithms. For the case of the NRTL equation, the GOP algorithm of Floudas and Visweswaran (1990, 1993) is used to guarantee obtaining ϵ-global convergence to the global minimum. For the UNIQUAC equation, a branch and bound algorithm based on that of Falk and Soland (1969) is used to guarantee convergence to the global solution. The computational results demonstrate the efficiency of both global optimization algorithms in solving a variety of challenging problems.

*Author to whom all correspondence should be addressed.

1 Introduction

A persistently difficult problem in chemical engineering is the phase and chemical equilibrium problem which is of crucial importance in several process separation applications. For conditions of constant temperature and pressure, a global minimum of the Gibbs free energy function describes the true equilibrium state. However, due to the presence of multiple solutions and the complexity of the models employed, all previous approaches have been unable to provide a guarantee of obtaining the global solution for the general equilibrium problem. Recently, McDonald and Floudas (1994a) proposed a global optimization approach that will find a global solution for the minimization of the Gibbs free energy function, when the liquid phase is modeled using the NRTL equation. McDonald and Floudas (1994b) also applied a global optimization algorithm when the liquid phase can be characterized by the UNIQUAC equation. The difficulty of finding the true equilibrium solution has stimulated much interest in the phase stability problem. This is because a solution obtained from the minimization of the Gibbs free energy can be tested for intrinsic thermodynamic stability by using the Gibbs tangent plane criterion, as first proposed by Gibbs (1873a, 1873b). It also recognizes the metastable region as unstable, a useful property in engineering applications.

Gautam and Seider (1979) used a phase–splitting algorithm in conjunction with the Rand method to improve the performance and reliability of their approach. Baker *et al.* (1982) proved the Gibbs tangent plane criterion for mixtures where the Gibbs free energy is a continuous first order function. They demonstrated the problems associated with conventional stability criteria when several solutions exist satisfying the condition of equal chemical potentials. Smith *et al.* (1993) have recently obtained the necessary and sufficient conditions for stability of systems where chemical reaction may or may not be taking place, using the Karush–Kuhn–Tucker (KKT) optimality conditions as the basis of their consideration.

The work of Michelsen (1982a, 1982b), provided the first efficient implementation of the tangent plane criterion. A two stage approach was proposed whereby the stability problem was used to generate initial points to be used in the search for a global minimum of the Gibbs free energy. Experience revealed that if the postulated solution is indeed thermodynamically unstable, the solutions obtained from the stability problem usually provide a good starting point for the new search. Sun and Seider (1994) also used a two stage approach, and employed a homotopy algorithm in an attempt to obtain the global solutions.

Swank and Mullins (1986) compared various methods for calculating liquid phase–splitting problems. The results showed that reliability could be increased but that there is no guarantee that phase equilibrium will be calculated correctly in all cases. Nagarajan *et al.* (1991a, 1991b) reformulated the stability approach replacing the mol numbers by mol densities, so that the Helmholtz free energy is the proper thermodynamic function describing equilibrium. Gupta *et al.* (1991) combined the phase equilibrium problem and the stability problem to avoid singular Jacobians. Their approach is guaranteed to converge to a stationary point. Eubank *et al.* (1992) integrate the Gibbs free energy surface for a single hypothetical phase, obtaining a maximum area rather than a minimum tangent plane distance. A maximum of three components and two phases may be postulated and convergence cannot be guaranteed if the solution lies at a composition bound.

Even though the stability problem has been effectively used to improve the chances of finding the true equilibrium solution corresponding to a global minimum of the Gibbs free energy, there is no guarantee that it will be obtained. It is usually assumed that if a postulated solution is found to be thermodynamically unstable, then a phase must be added or deleted. However, the true equilibrium solution may in fact be a solution with the same number of phases as the postulated one, but with a different distribution of the components within those phases.

In this work, it is shown how global solutions can be obtained for the phase stability problem for the case when nonideal liquid phases can be modeled using the NRTL or UNIQUAC equations. This is an important result because if a global approach shows that a solution satisfying the condition of equal chemical potentials is stable with respect to all possible perturbations, then global stability can be definitively asserted, i.e. the solution corresponds to a global minimum of the Gibbs free energy. Firstly, an introduction to the problem is supplied, including a brief derivation of the tangent plane stability criterion. The next two sections discuss how the formulations for the NRTL and UNIQUAC equations can be altered from their original nonconvex forms into problems with special structure. The NRTL can be transformed into a biconvex problem, while the UNIQUAC formulation is expressed as the difference of two convex functions, where the concave portion is separable. It will be shown how the recast formulations can be solved for ϵ-global optimality by using available global optimization algorithms. In the case of the NRTL equation, the GOP algorithm of Floudas and Visweswaran (1990, 1993) is used to obtain global solutions. For the UNIQUAC equation, the branch and bound algorithm of Falk and Soland (1969) is used to obtain global solutions to the reformulated problem. Examples are provided in both cases which demonstrate the success in generating the global solutions of the phase stability problem, regardless of starting point.

2 Problem Statement

Before discussing and deriving the tangent plane criterion, the motivation for its use is briefly outlined. This arises from consideration of the Gibbs free energy surface and the manner in which the tangents to this surface can describe the nature of equilibrium. Consider a binary system that is characterized by a single thermodynamic model, which is unspecified as yet, and it is assumed to be first order continuous. Then a plot such as the one shown in Figure 1 is obtained where the molar Gibbs free energy curve, $g(y)$, is plotted versus the mol fraction, y, of one of the components. The mol fraction of the second component is given by $1-y$. Suppose that a two–phase solution corresponding to a *local* (not global) minimum of the Gibbs free energy function has the mol fraction of component one in phase one denoted by z^1 and in phase two by z^2, with associated chemical potentials $\mu^0(z^1)$ and $\mu^0(z^2)$. Note that the superscripts refer to phases, not components. This local solution satisfies the necessary first order condition of equal chemical potentials, so that $\mu^0(z^1) = \mu^0(z^2)$. If the tangents to the Gibbs surface are drawn at z^1 and z^2, then these correspond to the tangent plane to the

Gibbs free energy surface $\mathcal{T}(z^1) = \mathcal{T}(z^2) = y_1\mu^0(z^1)$. This implies that points of common tangency reveal multiple phases. Note that the tangent line associated with this local solution lies above the Gibbs surface in a small region around $y \approx 0.6$, indicating thermodynamic instability. However, the situation for the solution corresponding to a global minimum is pictured in Figure 2 obtained for a different z^1 and z^2 than before. In this case, the common tangent lies completely below the Gibbs surface. For any mol fraction y that falls between z^1 and z^2, the hypothetical single liquid phase is unstable and will split into two phases with the compositions in each phase given by z^1 and z^2 respectively. The key characteristic is that if a tangent plane that lies completely below the Gibbs free energy surface does exist, then the equilibrium solution corresponding to the global minimum of the Gibbs free energy is given by the compositions at the points of tangency.

However, in the general multi–component, multi–phase problem there is no rigorous approach to determine where the tangent plane touches the Gibbs free energy surface so that it always lies below it. Rather, a point is picked on the composition space, which corresponds to some solution that satisfies the condition of equipotentials, and the tangent plane arising from this solution is checked to ensure that it lies below the Gibbs free energy surface for all feasible compositions. It will now be briefly shown why negative tangent plane distances reveal instability. Assume that the system in question is at constant temperature and pressure. Then the Gibbs free energy function is the thermodynamic quantity of interest. If the index set C represents the components i so that $C \equiv \{i\}$, then consider a single phase with mol fractions z_i and total mols n^0. An infinitesimal number of mols ϵ is split from the original phase to form two new phases, with the new phase having mol fractions y_i, and the original phase now containing $\mathrm{n}^0 - \epsilon$ mols. The change in the Gibbs free energy arising from this change is given as follows:

$$\begin{aligned}
\Delta G &= G(\epsilon) + G(\mathrm{n}^0 - \epsilon) - G(\mathrm{n}^0) \\
&= \sum_{i \in C} \epsilon\, y_i \mu_i(y) + G(\mathrm{n}^0) - \sum_{i \in C} \epsilon\, y_i \left.\frac{\partial G}{\partial \epsilon y_i}\right|_z - G(\mathrm{n}^0) \\
&= \sum_{i \in C} \epsilon\, y_i \left\{ \mu_i(y) - \mu_i^0(z) \right\}
\end{aligned}$$

If this energy change is positive for all feasible values of y, then the Gibbs energy of the postulated phase cannot be reduced by adding, deleting or changing the relative amounts of the various components in the postulated solution, so that it is seen to be stable. On the other hand, if the energy change is negative, then another solution must be sought which will have a lower value of the Gibbs free energy function.

Baker *et al.* (1982) and Smith *et al.* (1993) provide extensive proofs that a necessary and sufficient condition for a postulated solution to be an equilibrium one is that the tangent plane distance function, denoted $\mathcal{F}(y)$ be nonnegative *for all possible phases represented in the system*, with $\mathcal{F}(y)$ defined as follows:

$$\mathcal{F}(y) = \sum_{i \in C} y_i \left\{ \mu_i(y) - \mu_i^0(z) \right\} \tag{1}$$

where $\mu_i(y)$ and $\mu_i^0(z)$ represent the chemical potentials calculated at y and z respectively. The significance of the tangent plane criterion has been illustrated in Figures 1 and 2. The tangent plane distance function is defined as the distance between the Gibbs surface and the tangent plane constructed to this surface at z. This is summarized as follows:

- $g(y) = \sum_{i \in C} y_i \mu_i(y)$ Molar Gibbs surface (for a single hypothetical phase)
- $\mathcal{T}(y) = \sum_{i \in C} y_i \mu_i^0(z)$ Tangent plane to this surface at z
- $\mathcal{F}(y) = g(y) - \mathcal{T}(y)$ Tangent plane distance function

Clearly, if the tangent plane lies completely below the Gibbs surface as in Figure 2, then the postulated solution corresponds to a global minimum of the Gibbs free energy.

Previous approaches have concentrated on obtaining the stationary points of the tangent plane distance function, which reduce to solving the set of nonlinear equations:

$$\mu_i(y) - \mu_i^0(z) = K \tag{2}$$

subject to the feasibility constraints on y. If any of the solutions to this set of equations is negative, then the postulated solution is unstable and an improved solution with a lower Gibbs free energy must be sought. If all stationary points are found to be nonnegative, then it is assumed that the postulated solution is stable. However, there are a number of difficulties associated with this approach. Firstly, no guarantee of obtaining all stationary points can be provided so that even if no negative solutions are obtained, the postulated configuration may be unstable. Also, the solutions obtained from the stability problem are then used to initiate the search for a solution with a lower Gibbs free energy. However, there is no way of telling which stationary points correspond to the global solution, so that these guesses may in fact lead to local optima, or even infeasible solutions. Note that if homotopy continuation methods are employed in an attempt to locate all stationary points, no theoretical guarantee of identifying them can be provided, as the phase stability problem contains logarithmic terms. Such guarantees can only be made for polynomial systems of equations.

In this work, a global optimization approach is introduced. The tangent plane distance function is explicitly minimized. If a nonnegative global optimum solution is obtained, then the stability of the postulated solution is guaranteed. The optimization formulation for the phase stability problem, (S), is then given as:

$$\left.\begin{array}{ll} \min & \mathcal{F}(y) = \sum_{i \in C} y_i \left\{ \mu_i(y) - \mu_i^0(z) \right\} \\ s.t. & \sum_{i \in C} y_i = 1 \\ & 0 \le y_i \le 1 \end{array}\right\} \text{(S)}$$

Difficulties arise in obtaining global optimum solutions for (S) due to the complex and nonlinear nature of the models available to characterize $\mu_i(y)$ for nonideal phases. In this work, the situation for nonideal liquid phases that can be modeled using the NRTL and UNIQUAC equations is analyzed. The next two sections demonstrate (i) how the formulations can be altered from their original nonconvex forms into problems with special structure, and (ii) how deterministic global optimization methods can be employed to obtain global optima.

3 Application to the NRTL equation

3.1 Formulation of $\mathcal{F}(y)$

For conditions of constant temperature and pressure, the Gibbs free energy is the thermodynamic function that defines equilibrium for the system. The ideal molar Gibbs free energy, labeled g^I, for any mixture of components is given as:

$$\frac{g^I}{RT} = \sum_{i \in C} y_i \frac{\bar{g}_i}{RT} + \sum_{i \in C} y_i \ln y_i \tag{3}$$

where y_i represents the mole fraction of component i, and $\bar{g}_i$ is the molar Gibbs free energy of pure component i referred to some standard state, as yet undefined. For liquid phases, non–ideality is commonly predicted by using *excess* functions which describe the deviation of the system from ideal behavior. Renon and Prausnitz (1968) derived the following expression for g^E, the excess molar Gibbs free energy function:

$$\frac{g^E}{RT} = \sum_{i \in C} y_i \frac{\sum\limits_{j \in C} \tau_{ji} \mathcal{G}_{ji} y_j}{\sum\limits_{l \in C} \mathcal{G}_{li} y_l} = \sum_{i \in C} y_i \frac{\sum\limits_{j \in C} \tau_{ij} \mathcal{G}_{ij} y_j}{\sum\limits_{l \in C} \mathcal{G}_{lj} y_l} \tag{4}$$

where τ_{ij} are non-symmetric binary interaction parameters, $\mathcal{G}_{ij}$ are parameters which depend on another adjustable parameter, α_{ij} (with $\alpha_{ii} = 0$ and $\alpha_{ij} = \alpha_{ji}$). The relationship between these three parameters is given as $\mathcal{G}_{ij} = \exp\left(-\alpha_{ij}\tau_{ij}\right)$ so that $\mathcal{G}_{ij}$ can never be negative. It is possible to have negative τ_{ij}. This implies that there are three adjustable parameters per binary (τ_{ij},τ_{ji},α_{ij}).

The molar Gibbs free energy is given as the sum of the ideal portion and the excess portion:

$$\frac{g}{RT} = \frac{g^I}{RT} + \frac{g^E}{RT} \tag{5}$$

Substitution of Eqns. (3) and (4) into Eqn. (5) yields the following expression for the molar Gibbs free energy of a single hypothetical phase:

$$g(\boldsymbol{y}) = \sum_{i \in C} y_i \left\{ \Delta G_i^f + \ln y_i \right\} + \sum_{i \in C} y_i \frac{\sum\limits_{j \in C} \tau_{ij} \mathcal{G}_{ij} y_j}{\sum\limits_{l \in C} \mathcal{G}_{lj} y_l} \tag{6}$$

and the chemical potentials of each component are calculated as:

$$\mu_i(y) = \Delta G_i^f + \ln y_i + \frac{\sum\limits_{j\in C} \tau_{ji}\mathcal{G}_{ji}y_j}{\sum\limits_{j\in C} \mathcal{G}_{ji}y_j} + \sum_{j\in C} \frac{\mathcal{G}_{ij}y_j}{\sum\limits_{l\in C}\mathcal{G}_{lj}y_l}\left\{\tau_{ij} - \frac{\sum\limits_{l\in C}\tau_{lj}\mathcal{G}_{lj}y_l}{\sum\limits_{l\in C}\mathcal{G}_{lj}y_l}\right\} \quad \forall\, i \in C \tag{7}$$

where ΔG_i^f represents the Gibbs free energies of the pure components at the system temperature T, constructed so that the Gibbs energy content of the elemental species is zero at T. Notice that all quantities associated with the Gibbs free energy (such as $g(y)$, $\mu_i(y)$, $\mathcal{F}(y)$, ΔG_i^f) have now been made dimensionless by dividing by RT.

The tangent plane distance function can be written as:

$$\mathcal{F}(y) = g(y) - \sum_{i\in C} y_i\mu_i^0(z) \tag{8}$$

$$= \sum_{i\in C} y_i \left\{\Delta G_i^f + \ln y_i + \frac{\sum\limits_{j\in C}\tau_{ij}\mathcal{G}_{ij}y_j}{\sum\limits_{l\in C}\mathcal{G}_{lj}y_l} - \mu_i^0(z)\right\} \tag{9}$$

By finding the global minimum of $\mathcal{F}(y)$ over the convex constraint set of the phase stability problem (S), it is possible to determine whether the postulated solution represented by z is stable. If the global minimum of (S) is negative, then a solution with a lower Gibbs free energy must be sought by some other means. If a nonnegative value is obtained for the global minimum of $\mathcal{F}(y)$, then the solution is stable, and the postulated solution describes the equilibrium state.

There are a number of difficulties associated with obtaining the global solution of the function given in Eqn. (9). In order to demonstrate the structure of the stability problem, the convex terms of the tangent plane distance function, labeled $\mathcal{C}^N(y)$, are collected together as follows:

$$\mathcal{C}^N(y) = \sum_{i\in C} y_i \left\{\Delta G_i^f + \ln y_i - \mu_i^0(z)\right\} \tag{10}$$

Note that the terms $y_i \ln y_i$ are convex, and the remaining terms are linear. This implies that the objective function can now be written as:

$$\mathcal{F}(y) = \mathcal{C}^N(y) + \sum_{i\in C} y_i \frac{\sum\limits_{j\in C}\tau_{ij}\mathcal{G}_{ij}y_j}{\sum\limits_{l\in C}\mathcal{G}_{lj}y_l} \tag{11}$$

The nonconvexities in Eqn. (11) arise solely due to the excess Gibbs free energy term, and consist of a summation of terms that each involves a linear term times a linear fractional term.

3.2 Transformations and Partitioning

Before proceeding with the analysis, the following optimization problem is briefly discussed:

$$\begin{aligned} \min \quad & f(x,y) \\ s.t. \quad & h(x,y) = 0 \\ & g(x,y) \le 0 \\ & x \in X \ , \ y \in Y \end{aligned}$$

where X and Y are convex sets, and $f(x,y)$, $h(x,y)$ and $g(x,y)$ are presumed to be continuous and piecewise differentiable on $X \times Y$. Floudas and Visweswaran (1990, 1993) have proved ϵ-global convergence for problems that satisfy the following *Conditions (A)*:

- $f(x,y)$ and $g(x,y)$ are convex in x for all fixed y and convex in y for all fixed x,
- $h(x,y)$ is affine in x for all fixed y, and affine in y for all fixed x,
- X and $Y \subseteq V$ are nonempty, compact convex sets and a constraint qualification is satisfied, where $V \equiv \{\ y\text{: } h(x,y) = 0, g(x,y) \leq 0,$ for some $x \in X\}$.

By introducing new variables labeled $\mathcal{X}_i$, it is possible to change the nature of the nonconvexities of Eqn. (11) so that the GOP algorithm (Floudas and Visweswaran, 1990, 1993) can be applied to the phase stability problem:

$$\mathcal{X}_i = \frac{y_i}{\sum\limits_{j \in C} \mathcal{G}_{ji} y_j} \quad \forall\, i \in C \tag{12}$$

Substituting these variables into Eqn. (11) yields the following reformulated stability problem for the NRTL equation (S–N) given below:

$$\left.\begin{array}{ll} \min & \mathcal{F}(\boldsymbol{y}) = \mathcal{C}^N(\boldsymbol{y}) + \sum\limits_{i \in C} y_i \cdot \sum\limits_{j \in C} \mathcal{G}_{ij} \tau_{ij} \mathcal{X}_j \\ s.t. & \mathcal{X}_i \cdot \sum\limits_{j \in C} \mathcal{G}_{ji} y_j = y_i \quad \forall\, i\, \in C \\ & \sum\limits_{i \in C} y_i = 1 \\ \text{with} & Y \equiv \{\, y_i : 0 \leq\ y_i\ \leq\ 1 \quad \forall\, i\, \in C\} \end{array}\right\} \text{(S–N)}$$

Note that the constraints of Eqn. (12) have been rewritten so that they are of a bilinear form, rather than linear fractional.

(S–N) reveals that there is a natural partition of the variables into two distinct subsets to ensure that a convex subproblem remains if one of these subsets is held fixed. Suppose that the variables are partitioned so that the original mol number variables belong to the set of y variables (i.e. $y \leftarrow \{y_i\}$), and the new introduced variables belong to the set of x variables (i.e. $x \leftarrow \{\mathcal{X}_i\}$). Then *Conditions* (A) required by the GOP (Floudas and Visweswaran, 1990, 1993) to guarantee ϵ-global convergence are satisfied. Examining the new formulation reveals that if the y variables are held constant, then a linear objective function results subject to a linear set of constraints. If the $\mathcal{X}$ variables are held fixed, then a convex objective function is obtained subject to a linear set of equality constraints. Thus, *Conditions (A)* of the GOP are satisfied. The GOP algorithm proceeds by iterating between the primal problem, which supplies upper bounds on the global solution, and a set of relaxed dual subproblems which yield lower bounds on the global solution. The relaxed dual subproblems are derived through consideration of duality theory. These subproblems will now be discussed.

3.3 The Primal Problem

The primal problem (P) is obtained by fixing the y variables such that $\boldsymbol{y} = \boldsymbol{y}^K \in Y$ at some iteration K. To ensure feasibility, the mol fraction constraint ($\sum_i y_i^K = 1$) must be satisfied. (P) is explicitly given as:

$$\begin{aligned} \min_{\mathcal{X}} \quad & \mathcal{C}^N(\boldsymbol{y}^K) + \sum_{i \in C} y_i^K \cdot \sum_{j \in C} \mathcal{G}_{ij} \tau_{ij} \mathcal{X}_j \\ s.t. \quad & \mathcal{X}_i \cdot \sum_{j \in C} \mathcal{G}_{ji} y_j^K = y_i^K \qquad \forall \quad i \in C \end{aligned}$$

Note that (P) has a linear objective function and constraints in the variables $\mathcal{X}_i$, and is therefore convex. Its solution provides an upper bound on the global solution because it represents a restriction of the original problem. The definitions of the $\mathcal{X}$ variables form a square set of equality constraints so that (P) is simply a function evaluation.

3.4 The Relaxed Dual Problem

The primal problem yields an upper bound on the global solution. The relaxed dual subproblems will yield valid lower bounds. A more detailed treatment of the theory can be found in Floudas and Visweswaran (1990, 1993) and in McDonald and Floudas (1994a).

3.4.1 Formulation of the Lagrange function

The Lagrange function for use in the relaxed dual problem will supply underestimators of the Gibbs surface in partitions of the feasible region. If the following steps are performed:

(i) Construct the Lagrange function from (S–N) as $L(\mathcal{X}, y, \lambda) = f(\mathcal{X}, y) + \lambda^T h(\mathcal{X}, y)$,

(ii) Collect the $\mathcal{X}$ variable terms together,

(iii) Use the KKT conditions from the primal problem,

(iv) Construct a relaxation of the Lagrange function that allows for rectangular partitioning,

(v) Augment the set of $\mathcal{X}$ variables with the new set denoted as $\hat{\mathcal{X}}$,

then the Lagrange function can be written as:

$$L(\hat{\mathcal{X}}, y, \lambda^K) = \sum_{i \in C} \sum_{j \neq \bar{\imath}} \hat{\mathcal{X}}_{ij} \left\{ \left\{ \mathcal{G}_{ji} \left[\tau_{ji} + \lambda^K_{\mathcal{X}_i} \right] - \mathcal{G}_{\bar{\imath}i} \left[\tau_{\bar{\imath}i} + \lambda^K_{\mathcal{X}_i} \right] \right\} \cdot \left\{ y_j - y_j^K \right\} \right\} + \mathcal{C}^N(\boldsymbol{y}) - \sum_{i \in C} y_i \lambda^K_{\mathcal{X}_i} \quad (13)$$

where $\bar{\imath}$ is the last member of the set of components so that $y_{\bar{\imath}} = 1 - \sum_{i \in CR} y_i$, with $CR \equiv C \setminus \{\bar{\imath}\}$. The augmented set of variables is defined for each $i \in C$ as $\hat{\mathcal{X}}_{ij} = \mathcal{X}_i \ \forall \ j \in CR$. The derivatives of Eqn. (13) with respect to the $\mathcal{X}$ variables are the qualifying constraints of the GOP, given by:

$$\hat{g}_{ij}(\boldsymbol{y}) = \nabla_{\hat{\mathcal{X}}_{ij}} L(\hat{\mathcal{X}}, y, \lambda^K) = \left\{ \mathcal{G}_{ji} \left[\tau_{ji} + \lambda^K_{\mathcal{X}_i} \right] - \mathcal{G}_{\bar{\imath}i} \left[\tau_{\bar{\imath}i} + \lambda^K_{\mathcal{X}_i} \right] \right\} \cdot \left\{ y_j - y_j^K \right\} \ \forall \ i \in C, j \in CR \quad (14)$$

The number of connected variables is the minimum number of $\mathcal{X}$ or y variables that interact bilinearly so that $N_{CV} = |C| - 1$. Note that each qualifying constraints consists of a *single* term $(y_j - y_j^K)$, allowing the y variable space to be partitioned into simple orthogonal regions. This is described in the next section.

3.4.2 Partitioning of the y variable space

At any given iteration, the current regional lower and upper bounds for the y variables are $\{\mathcal{L}_{y_i}^R\}$ and $\{\mathcal{U}_{y_i}^R\}$ respectively. This parent region is then divided into $2^{N_{CV}}$ subregions by the current point, $\{y_i^K\}$. The lower and upper bounds for these subregions are labeled $\{\mathcal{L}_{y_i}^B\}$ and $\{\mathcal{U}_{y_i}^B\}$, respectively. The set of $2^{N_{CV}}$ combinations is denoted CB. The parameter $\{s_i^{B_l}\}$, defined over $CR \times CB$, gives the subregion and the bounds as follows:

$$\left.\begin{array}{llllllll} \text{If} & s_i^{B_l} = +1 & \text{then} & (y_i - y_i^K) \geq 0 & \Rightarrow & \mathcal{L}_{y_i}^B = y_i^K & , & \mathcal{U}_{y_i}^B = \mathcal{U}_{y_i}^R \\ \text{If} & s_i^{B_l} = -1 & \text{then} & (y_i - y_i^K) \leq 0 & \Rightarrow & \mathcal{L}_{y_i}^B = \mathcal{L}_{y_i}^R & , & \mathcal{U}_{y_i}^B = y_i^K \end{array}\right\} \quad \forall \quad i \in C$$

A relaxed dual subproblem is solved within each of these subregions to generate a lower bound on the global solution which is valid for that particular region. Successive refinements of the feasible region will then lead to convergence to the global solution. A detailed discussion of the details of the algorithm can be found in McDonald and Floudas (1994a).

Bounds on the set of $\mathcal{X}$ variables are required for the relaxed dual problem. The $\mathcal{X}$ variables as defined by Eqn. (12) are pseudolinear, that is, they are convex *and* concave. Thus there will be one global minimum, denoted $\mathcal{L}_{\mathcal{X}_i}$, and one global maximum, denoted $\mathcal{U}_{\mathcal{X}_i}$, as defined below:

$$\left.\mathcal{L}_{\mathcal{X}_i} = \frac{\mathcal{L}_{y_i}^B}{\mathcal{L}_{y_i}^B + \sum\limits_{j \neq i} \mathcal{G}_{ji}\mathcal{U}_{y_j}^B} \quad \text{and} \quad \mathcal{U}_{\mathcal{X}_i} = \frac{\mathcal{U}_{y_i}^B}{\mathcal{U}_{y_i}^B + \sum\limits_{j \neq i} \mathcal{G}_{ji}\mathcal{L}_{y_j}^B} \quad \right\} \quad \forall\, i \in C \qquad (15)$$

The proof of the above result is supplied by McDonald and Floudas (1994a).

3.4.3 Setting the bounds on the $\mathcal{X}$ variables

The $\mathcal{X}$ variables are set at their lower or upper bounds for the current iteration K, and the set of previous iterations, denoted $PL(\bar{K})$. This will depend both on the box region and the sign of the premultiplying constant term of the qualifying constraints given by Eqns. (14). For the current iteration, the sign of the box constraint terms are already set for any given box region by $s_i^{B_l}$. If the combined sign of the terms are positive, then the corresponding $\mathcal{X}$ variable should be set to its lower bound, while if it is negative, the $\mathcal{X}$ variable must be set at its upper bound to yield a valid underestimation of the original problem. For the previous iterations, the combined sign is evaluated through the premultiplying terms of Eqns. (14) evaluated at iteration $\bar{K}$ and the sign of the quantity $y_i^K - y_i^{\bar{K}}$, which validly determines the sign of $y_i - y_i^{\bar{K}}$ in the current region. The detailed steps of the algorithm are outlined in Appendix A.

3.5 Examples for the NRTL

Before describing the examples, it is necessary to make the following comments in relation to them:

(i) For examples where reaction does not occur, the Gibbs free energy of formation term for the vapor phase is removed through the following approximation:

$$\Delta G_i^{L,f} = \Delta G_i^{V,f} + RT \ln P_i^S \;\forall\; i \;\in C \tag{16}$$

In cases where the data has been obtained independently of the vapor phase, the saturated pressure term can also be eliminated to minimize the dependence on physical data.

(ii) The postulated solutions used to test for stability are obtained from minimizing the Gibbs free energy function, either locally or from the global optimization approach of McDonald and Floudas (1994a). These solutions have a separate notation associated with them. The set of phases is denoted $P \equiv P_L \cup P_V \equiv \{k\}$, where the liquid phases are designated $L_k \subseteq P_L$, and the vapor phase is denoted as $V \equiv P_V$. For any postulated solution, the mol fractions of each component i in some phase k are given by z_i^k, so that $\sum_i z_i^k = 1 \;\forall\; k \in P$. The parameter ϕ^k corresponds to the fraction of total mass in phase k, so that $\sum_k \phi^k = 1$. In the results tables that follow, y_i^* is the mol vector at a global solution, with $\mathcal{F}^*$ being the corresponding tangent plane distance function. The numbers in parentheses below $\mathcal{F}^*$ show the results of using the NLP solver MINOS5.4 to solve the original nonconvex formulations from 100 randomly chosen starting points, with the first number corresponding to the number of failures in obtaining a negative tangent plane distance function when the postulated solution is a non-equilibrium one, and the second number showing how many times the global solution was obtained. N_I is the number of iterations, with the number in parentheses corresponding to the iteration number at which the tangent plane distance function becomes negative. The number in parentheses reported under the cpu time for the problems corresponds to the total cpu time consumed before a negative tangent plane distance is obtained. N_F is the percentage of solution nodes that are fathomed because the lower bound lies above the best current upper bound.

(iii) All computational runs were performed on a Hewlett Packard 9000/730 machine. The algorithm is implemented in C as the package **GLOPEQ** (GLObal OPtimization for the Phase EQuilibrium problem) which is also capable of minimizing the Gibbs free energy function using the same algorithms employed for the phase stability problem. The solver MINOS5.4 is accessed as a subroutine. All cpu times reported represent the total *real time* taken to solve any given phase stability problem to ϵ-global optimality, where tolerances of $\epsilon = 10^{-6}$ for the NRTL equation and $\epsilon = 10^{-5}$ for the UNIQUAC equation were found to give a more than satisfactory criterion of convergence.

Example 1: n-Butyl-Acetate – Water

This example is small but challenging and is analyzed here at four different feed conditions. There are two components and a maximum of two liquid phases, so that Comment (i) above applies. The binary parameters of the system are given by Heidemann and Mandhane (1973) as:

$$\tau_{12} = 3.00498 \ , \ \tau_{21} = 4.69071 \ , \ \alpha_{12} = 0.391965$$

The explicit formulation for the phase stability problem expressed in terms of the original and transformed variables is as follows:

$$\begin{aligned} \min \quad & y_1 \ln y_1 + y_2 \ln y_2 - y_1 \mu_1^0(z) - y_2 \mu_2^0(z) + \mathcal{G}_{12} \tau_{12} y_1 \mathcal{X}_2 + \mathcal{G}_{21} \tau_{21} y_2 \mathcal{X}_1 \\ s.t. \quad & \mathcal{X}_1 \cdot \{y_1 + \mathcal{G}_{21} y_2\} = y_1 \\ & \mathcal{X}_2 \cdot \{\mathcal{G}_{12} y_1 + y_2\} = y_2 \\ & y_1 + y_2 = 1 \quad , \quad 0 \leq y_1, y_2 \leq 1 \end{aligned}$$

Note that there are two bilinear terms in the objective function, and two bilinear constraints, which make the problem nonconvex. The Lagrangian constructed from any given primal problem at some iteration K for use in the relaxed dual subproblems is then:

$$\begin{aligned} L(\mathcal{X}, y, \lambda^K) \ = \ & y_1 \ln y_1 + y_2 \ln y_2 - y_1 \left[\mu_1^0(z) + \lambda_1^K\right] - y_2 \left[\mu_2^0(z) + \lambda_2^K\right] \\ & + \{y_1 - y_1^K\} \cdot \{\mathcal{X}_1 \{\lambda_1^K - \mathcal{G}_{21} [\tau_{21} + \lambda_1^K]\} + \mathcal{X}_2 \{\mathcal{G}_{12} [\tau_{12} + \lambda_2^K] - \lambda_2^K\}\} \end{aligned}$$

y_1 is the only variable that interacts bilinearly with the $\mathcal{X}$ variable set, so that $N_{CV} = 1$ for this example.

Geometric Interpretation

The performance of the GOP will now be illustrated for the case of an equimolar feed, so that the total number of mols of each component is given as $n_1^T = n_2^T = 0.5$. The test candidate phase will be a single liquid phase so that $z_1 = z_2 = 0.5$. These values of z substituted into Eqn. (7) yield $\mu_1^0(z) = -0.06391$ and $\mu_2^0(z) = 0.02875$. The objective function is plotted in Figure 3 and reveals a nonconvex curve with multiple stationary and inflection points. In fact, there are two local minima, one of which is the global one, a local maximum and several inflection points, and the values of y_1 where these occur (excluding the maxima at the boundaries of the feasible region) are given in Table 1. A local solver will converge at best to a local minimum, with no guarantee of obtaining the global solution. For this case, if the global solution is not obtained, then all the other stationary points yield a nonnegative objective function value, which would lead to the erroneous conclusion that the single liquid phase is stable. In fact, when solving this problem using MINOS5.4, only 29 of 100 randomly selected starting points gave the global solution. This clearly demonstrates the difficulties associated with application of the tangent plane stability criterion and highlights the need for a global optimization approach. The manner in which the GOP algorithm proceeds is now demonstrated for the first iteration.

Iteration 1: Choose an initial point of $y_1^1 = y_2^1 = 0.5$ which gives an upper bound of $\mathcal{F}(y^1) = 0$. The parent region is divided in two, and a relaxed dual subproblem is solved in each.

Region 1: The box bounds are: $0.5 \leq y_1 \leq 1.0$ (and hence $0.0 \leq y_2 \leq 0.5$). This implies that $(y_1 - y_1^1) \geq 0$. Solving the relaxed dual problem in this region yields a global solution of $y_1^* = 0.7788$ with a corresponding lower bound of $\mu_1^* = -0.1861$.

Region 2: The box bounds are: $0.0 \leq y_1 \leq 0.5$ (and hence $0.5 \leq y_2 \leq 1.0$). This implies that $(y_1 - y_1^1) \leq 0$. The global solution of the relaxed dual is $y_1^* = 0.1910$ with a corresponding lower bound of $\mu_2^* = -0.2469$. The underestimators for Regions 1 and 2 are drawn in Figure 4.

At the second iteration, Region 2 of Iteration 1 yields the next parent region, so that again 2 relaxed dual subproblems are solved to give two additional lower bounds. The algorithm proceeds in this way until the infimum of all remaining lower bounds is within ϵ of the current best upper bound. For this particular problem, convergence occurs after 12 iterations. The total time taken by the algorithm was 0.06 cpu sec, and 8 nodes were fathomed. The actual solution is given in Table 2. Note also that $\mathcal{F}^*$ becomes negative at an early stage of the algorithm so that it could be terminated because the postulated equilibrium solution is clearly unstable.

Other feed conditions

The algorithm was also tested for three other feed conditions, with different values of $\{n_i^T\}$. The stability test was initiated in all cases by a single liquid phase solution, with $z_i = n_i^T / \sum_j n_j^T \ \forall\ i$. The only difference between the formulations will then be the values calculated for $\mu_i^0(z)$. This leads to negative tangent plane distances in all cases and these results are also shown in Table 2. The first and last feed conditions ($n_1^T = 0.5$ and $n_1^T = 0.65$) are seen to be the most difficult. The local searches show a large number of failures in terms of predicting that the one phase solution is unstable. This is also reflected in the fact that a negative tangent plane distance is not obtained until the fourth iteration in both cases. On the other hand, the middle two feed conditions are much less challenging, with the local searches showing no failures in predicting instability. However, for $n_1^T = 0.1$, the global solution was obtained only 5 times out of 100.

Local LL solution

When the Gibbs free energy is minimized to attempt to obtain the global solution, the four feed conditions yield a strong local LL solution which satisfies the first order conditions of equal chemical potentials. This solution is given in Table 3 and can be used to test the algorithm. The mol fractions in the two phases are the same for all four feed conditions as they lie along the same tieline so that only the phase fractions differ. Obviously the tangent plane distance function is negative and a plot of the Gibbs surface and the tangent plane is provided in Figure 1. As for the illustrative example, notice that if a local solver converges to a stationary point other than the global minimum, then it will incorrectly confirm a false equilibrium solution. The global minimum is at $y_1^* = 0.59425$ with $\mathcal{F}(y^*) = -0.0007$, indicating instability of the local LL solution. The algorithm takes 30 iterations to converge to this solution using a total of 0.15 cpu sec, while 45% of the nodes were fathomed.

Global LL solution

All four feed conditions share the same mol fractions for the equilibrium solution corresponding to a global minimum of the Gibbs free energy, and these are also supplied in Table 3. The postulated global solution will obviously yield a nonnegative tangent plane distance over the full mol fraction space and this is pictured in Figure 2 where the tangent plane lies below the Gibbs surface over the feasible composition range. For a starting point of $y_1^1 = 0.75$, the global solution of zero is obtained after 36 iterations with the algorithm consuming a total of 0.16 cpu sec, while 43% of the nodes were fathomed. The time taken to verify the equilibrium solution is not significantly greater than that taken to establish instability for the other non-equilibrium postulated solutions.

Example 2: Toluene – Water – Aniline

This example is taken from Castillo and Grossmann (1981) and features three components at a temperature of 298K and a pressure of 1 atm. Bender and Block (1975) supply the parameters for this example and these are shown in Table 4. The phase rule indicates that there are a maximum of three phases. Paules and Floudas (1989) found that this example displayed troublesome characteristics in terms of convergence to the trivial solution. It demonstrates why the stability analysis is such a valuable tool because by solving the stability problem for a postulated trivial solution, there is the possibility of obtaining a negative tangent plane distance indicating that it is false.

Starting with a trivial solution, the global solution for the given feed conditions is supplied in Table 5. The global solution is obtained after 16 iterations with a total time of 0.18 cpu sec. Note that the tangent plane distance function becomes negative at the first iteration, indicating instability after only 0.001 cpu sec.

If the equilibrium solution corresponding to a global minimum of the Gibbs free energy is tested for stability, the tangent plane distance function will of course be nonnegative over the complete feasible region. In this case the global solution of zero is obtained after 85 iterations and the GOP algorithm takes a total time of 0.94 sec. In addition, 68% of the nodes were fathomed.

Example 3: *n*-Propanol – Water – Butanol

This system was first studied by Block and Hegner (1976) in their study of three phase distillation towers. It contains one partially miscible pair between water and *n*-butanol. The required binary parameters are given in Table 6 and it should be noted that these are independent of temperature, so that consideration of a vapor phase is meaningless. Walraven and Rompay (1988) also studied this example for a variety of feed conditions to test their phase splitting algorithm, and two of these source feeds were used to examine the performance of the global optimization algorithm:

$$\begin{aligned} \text{Condition (i):} \quad \{n_i^T\} &\equiv \{0.160, 0.800, 0.040\} \\ \text{Condition (ii):} \quad \{n_i^T\} &\equiv \{0.052, 0.800, 0.148\} \end{aligned}$$

Condition (i) corresponds to a relatively easy example that lies within the immisiscibility region, while Condition (ii) lies close to the plait point, and is therefore very challenging.

A local solver will not be able to guarantee obtaining the global solution from any given starting point. The results for Condition (i) are shown in Table 7, for both the trivial solution and the global solution as the postulated equilibrium solutions to be tested for stability. With a one phase solution postulated, there were no failures by the local solver in predicting instability although the global solution to the stability problem was only obtained 31 times out of 100 randomly selected starting points. Table 8 shows the results for Condition (ii) where the difficulty of the problem is reflected in the increased computer time required to establish stability. There were also a large number of failures (60 out of 100) when the stability problem was solved locally using MINOS5.4. Notice that the time required to verify instability is very small. Obviously, as soon as a negative tangent plane distance is found, the algorithm can be stopped. However, for the stable solutions the cpu time required to confirm an equilibrium solution is more punitive. It should be noted that the iteration at which the tangent plane distance function becomes negative occurs in the first iterations with a correspondingly low cpu usage. This will have important implications when the tangent plane criterion is used to test solutions obtained from the minimization of the Gibbs free energy because the concern is determining if this distance is negative.

4 Application to the UNIQUAC Equation

4.1 Formulation of $\mathcal{F}(y)$

Anderson and Prausnitz (1978) proposed the following expression for the excess Gibbs free energy:

$$\frac{g^E}{RT} = \sum_{i \in C} y_i \ln \frac{\phi_i}{y_i} + \frac{z}{2} \sum_{i \in C} q_i y_i \ln \frac{\theta_i}{\phi_i} - \sum_{i \in C} q_i' y_i \ln \left(\sum_{j \in C} \theta_j' \tau_{ji} \right) \tag{17}$$

where r_i, q_i and q_i' are pure component structural parameters, τ_{ij} is a binary interaction parameter, z is a lattice coordination number, and ϕ_i, θ_i and θ_i' defined as follows:

$$\begin{aligned} \phi_i &= \frac{r_i y_i}{\sum\limits_{j \in C} r_j y_j} \quad \forall \ i \in C \\ \theta_i &= \frac{q_i y_i}{\sum\limits_{j \in C} q_j y_j} \quad \forall \ i \in C \\ \theta_i' &= \frac{q_i' y_i}{\sum\limits_{j \in C} q_j' y_j} \quad \forall \ i \in C \end{aligned}$$

Collecting the terms involving ϕ_i and substitution of Eqns. (17) and (3) into Eqn. (5) leads to the following expression for the (dimensionless) molar Gibbs free energy:

$$g(\boldsymbol{y}) = \sum_{i \in C} y_i \left\{ \Delta G_i^f + \left[1 - \frac{z}{2} q_i\right] \ln \phi_i + \frac{z}{2} q_i \ln \theta_i - q_i' \ln \sum_{j \in C} \theta_j' \tau_{ji} \right\} \tag{18}$$

The chemical potentials for each component are defined as:

$$\begin{aligned} \mu_i(\boldsymbol{y}) \;&=\; \Delta G_i^f + \left[1 - \frac{z}{2} q_i\right] \ln \phi_i + \frac{z}{2} q_i \ln \theta_i + l_i - \frac{\phi_i}{y_i} \sum_{j \in C} l_j y_j \\ &\quad + q_i' - q_i' \ln \sum_{j \in C} \tau_{ji} \theta_j' - q_i' \sum_{j \in C} \frac{\tau_{ij} \theta_j'}{\sum\limits_{l \in C} \theta_l' \tau_{lj}} \end{aligned} \tag{19}$$

where l_i is given as:

$$l_i = \frac{z}{2} \cdot (r_i - q_i) - (r_i - 1) \quad \forall\, i \in C \tag{20}$$

In addition, the following new parameter is introduced:

$$z_i^R = \frac{\frac{z}{2} q_i - 1}{r_i} \quad > 0 \quad \forall \; i \in C \tag{21}$$

This parameter is always positive. If the terms involving ϕ_i, θ_i and θ_i' are fully expanded, then the tangent plane distance function for the UNIQUAC equation is obtained by substituting Eqn. (18) into Eqn. (8) to yield:

$$\mathcal{F}(\boldsymbol{y}) = \sum_{i \in C} y_i \left\{ \Delta G_i^f - z_i^R r_i \ln \frac{r_i y_i}{\sum\limits_{j \in C} r_j y_j} + \frac{z}{2} q_i \ln \frac{q_i y_i}{\sum\limits_{j \in C} q_j y_j} - q_i' \ln \frac{\sum\limits_{j \in C} q_j' \tau_{ji} y_j}{\sum\limits_{j \in C} q_j' y_j} - \mu_i^0(\boldsymbol{z}) \right\} \tag{22}$$

$\mathcal{F}(\boldsymbol{y})$ as defined above is clearly nonconvex. McDonald and Floudas (1994b) present various transformations and properties that allow this function to be expressed as the difference of two convex functions where the concave portion is separable. The results are summarized in the foregoing, but firstly, new parameters are introduced to aid in this process, defined as follows:

$$z_M^R \;=\; \min_i \{z_i^R\} \tag{23}$$

$$z^A \;=\; z_M^R + \sum_{i \in C} [z_i^R - z_M^R] \tag{24}$$

$$z_i^B \;=\; \sum_{j \neq i} \left[z_j^R - z_M^R\right] \qquad \forall \; i \in C \tag{25}$$

$$\varphi_i \;=\; q_i' + r_i\, [\, z_i^R + z_i^B\,] \qquad \forall \; i \in C \tag{26}$$

These new parameters allow the convex portion of the reformulated tangent plane distance function to be defined as:

$$\mathcal{C}^U(\boldsymbol{y}) \;=\; \sum_{i \in C} y_i \left\{ \Delta G_i^f - \mu_i^0(\boldsymbol{z}) - z_i^R r_i \ln r_i \right\}$$

$$+ \quad z^A \cdot \sum_{i \in C} r_i y_i \ln \sum_{i \in C} r_i y_i + \sum_{i \in C} z_i^B r_i y_i \ln \frac{y_i}{\sum\limits_{j \in C} r_j y_j}$$

$$+ \quad \frac{z}{2} \sum_{i \in C} q_i y_i \ln \frac{q_i y_i}{\sum\limits_{j \in C} q_j y_j} + \sum_{i \in C} q_i' y_i \ln \sum_{i \in C} q_i' y_i + \sum_{i \in C} q_i' y_i \ln \frac{y_i}{\sum\limits_{j \in C} q_j' \tau_{ji} y_j}$$

The reformulated stability problem for the UNIQUAC equation (S–U) can then be written:

$$\left.\begin{array}{ll} \min & \mathcal{F}(\boldsymbol{y}) = \mathcal{C}^U(\boldsymbol{y}) - \sum\limits_{i \in C} \varphi_i \, y_i \ln y_i \\ s.t. & \sum\limits_{i \in C} y_i = 1 \\ \text{with} & y \in Y \equiv \{y_i : 0 \leq \; y_i \; \leq \; 1 \quad \forall \; i \; \in C\} \end{array}\right\} \text{(S–U)}$$

This objective function is composed of the difference of two convex functions, where the convex function that is subtracted is separable in y_i, and is minimized over the convex set Y. This structure will be fully exploited in solving (S–U).

4.2 Branch and Bound Algorithm

For problems of similar structure to (S–U), a branch and bound algorithm was proposed by Falk and Soland (1969), which forms the basis of the algorithm used in this work. The basic idea is to successively refine the feasible region, solving convex subproblems in these subregions, and thus generating a nondecreasing subsequence of lower bounds that will converge on a global solution of (S–U).

4.2.1 Generating convex underestimators of $\mathcal{F}(y)$

For any given partition of the feasible region defined as:

$$\mathcal{L}_{y_i}^B \; \leq \; y_i \; \leq \; \mathcal{U}_{y_i}^B \qquad \forall \;\; i \in C \tag{27}$$

then a valid lower bound on the objective function is supplied by the convex envelope of $\mathcal{F}(\boldsymbol{y})$ defined in (S–U). The convex envelope of the separable concave term $-y_i \ln y_i$ is denoted $\Psi_i(y_i)$, and is simply the affine function that joins the endpoints for y_i as defined by Eqn. (27):

$$\Psi_i(y_i) = -\mathcal{L}_{y_i}^B \ln \mathcal{L}_{y_i}^B + \left[\frac{\mathcal{L}_{y_i}^B \ln \mathcal{L}_{y_i}^B - \mathcal{U}_{y_i}^B \ln \mathcal{U}_{y_i}^B}{\mathcal{U}_{y_i}^B - \mathcal{L}_{y_i}^B} \right] \left[y_i - \mathcal{L}_{y_i}^B \right] \quad \forall \;\; i \in C \tag{28}$$

Then the convex envelope of the concave function will be given by the sum of these individual affine functions. The following problem will then yield the convex envelope of $\mathcal{F}(\boldsymbol{y})$ and provides a valid underestimation of the global solution in the current region:

$$\left.\begin{array}{ll} \min & \mathcal{C}^U(y) + \sum_{i\in C} \varphi_i \Psi_i(y_i) \\ s.t. & \sum_{i\in C} y_i \;=\; 1 \\ & \mathcal{L}^B_{y_i} \;\leq\; y_i \;\leq\; \mathcal{U}^B_{y_i} \end{array}\right\}\text{(UES)}$$

For successive refinements of the feasible region, the lower bound supplied by (UES) will be tighter than that supplied by any of its predecessor nodes, creating a nondecreasing subsequence of lower bounds on the global solution. A local solution to (UES) is a global one.

4.2.2 Partitioning scheme for the y variable space

The notation in this section is the same as for the NRTL equation. As discussed by McDonald and Floudas (1994b), N_P hyperplanes are chosen to partition the current region with $1 \leq N_P \leq N_{CV}$, and $N_{CV} = |C| - 1$. N_P is a user specified parameter. The larger it is, the tighter will be the bounds created in a given region, but the number of subproblems solved for that iteration will be increased. Thus, 2^{N_P} box regions are created at every iteration, and an underestimating subproblem of type (UES) is solved in each to generate a valid lower bound on the global solution.

The current region is partitioned along the N_P edges with the largest distances, labeled δ_i, between the concave function and its convex envelope evaluated at $\boldsymbol{y}^K$. Horst and Tuy (1990) proved that the algorithm used in this work (which allows N_P to vary) converges finitely to an ϵ-global global solution of (S–U) if the subdivision rule just described is used.

The parameter $\mathcal{H}_i$ is used to decide if the current region will be partitioned along the facet of the n-rectangle involving y_i. If $\mathcal{H}_i = 1$, then the side of the n-rectangle associated with y_i will be partitioned, while if $\mathcal{H}_i = 0$, then it will not. This is summarized below:

$$\left.\begin{array}{llllll} \text{If} & s_i^{B_l}\cdot\mathcal{H}_i = +1 & \text{then} & (y_i - y_i^K) \geq 0 & \Rightarrow & \mathcal{L}^B_{y_i} = y_i^K \;,\; \mathcal{U}^B_{y_i} = \mathcal{U}^R_{y_i} \\ \text{If} & s_i^{B_l}\cdot\mathcal{H}_i = -1 & \text{then} & (y_i - y_i^K) \leq 0 & \Rightarrow & \mathcal{L}^B_{y_i} = \mathcal{L}^R_{y_i} \;,\; \mathcal{U}^B_{y_i} = y_i^K \\ \text{If} & s_i^{B_l}\cdot\mathcal{H}_i = \;\;\,0 & \text{then} & & & \mathcal{L}^B_{y_i} = \mathcal{L}^R_{y_i} \;,\; \mathcal{U}^B_{y_i} = \mathcal{U}^R_{y_i} \end{array}\right\}\;\forall\, i\in C \;,\; j \in CR$$

Some key characteristics of the algorithm are:

- Only one underestimating function is required per node.
- The current region can be partitioned using a variable number of hyperplanes.
- Each subproblem is unconstrained, except for the simple box bounds on the variables.

It proceeds by solving (S) locally with $\mathcal{F}(y)$ given by Eqn. (22) to give an upper bound on the global solution. The current region is then partitioned by hyperplane(s) passing through the current point, and 2^{N_P} subproblems of type (UES) are solved to yield a lower bound on the global solution in that particular subregion. If these solutions lie above the best upper bound, they are fathomed; otherwise they are added to the set of solution nodes. Then, the infimum of all available lower bounds is chosen as the node for the next iteration, so that the mol fraction solution associated with this node becomes the current point. Before returning to solve (S) locally, a check for convergence is done. The detailed steps of the branch and bound algorithm are presented in Appendix B.

4.3 Examples for the UNIQUAC equation

The same comments that were made in Section 3.5 are also applicable here.

Example 4: Toluene – Water

This first example is taken from Lantagne *et al.* (1988) where the modified version of the UNIQUAC equation is used, as the system contains water. There are a maximum of two phases, both assumed to be liquid, and the pure component structural data as well as their associated parameters introduced to change the form of the objective function are given in Table 9. The two binary interaction parameters are supplied as:

$$\tau_{12} = 0.09867 \ , \ \tau_{21} = 0.59673$$

The following definitions are also required:

$$\begin{aligned} z_M^R &= \min \{ \ z_1^R, z_2^R \ \} \\ &= \ z_1^R \ = 3.53316 \end{aligned}$$

$$\begin{aligned} z^A &= z_M^R + (z_1^R - z_M^R) + (z_2^R - z_M^R) \\ &= \ z_2^R \ = 6.52174 \end{aligned}$$

This allows the convex portion of the objective function to be written as:

$$\begin{aligned} \mathcal{C}^U(y_1, y_2) &= y_1 \left[-\mu_1^0(z) - z_1^R r_1 \ln r_1 \right] + y_2 \left[-\mu_2^0(z) - z_2^R r_2 \ln r_2 \right] \\ &+ \ z^A \left[r_1 y_1 + r_2 y_2 \right] \ln \left[r_1 y_1 + r_2 y_2 \right] + z_1^B r_1 y_1 \ln \frac{y_1}{r_1 y_1 + r_1 y_2} \\ &+ \ \frac{z}{2} q_1 y_1 \ln \frac{q_1 y_1}{q_1 y_1 + q_2 y_2} + \frac{z}{2} q_2 y_2 \ln \frac{q_2 y_2}{q_1 y_1 + q_2 y_2} \\ &+ \ \left[q_1' y_1 + q_2' y_2 \right] \ln \left[q_1' y_1 + q_2' y_2 \right] + q_1' y_1 \ln \frac{y_1}{q_1' y_1 + \tau_{21} q_2' y_2} + q_2' y_2 \ln \frac{y_2}{\tau_{12} q_1' y_1 + q_2' y_2} \end{aligned}$$

The explicit separable D.C. formulation is given as follows:

$$\begin{aligned} \min \quad & \mathcal{C}^U(y_1, y_2) - \varphi_1 \left[y_1 \ln y_1 \right] - \varphi_2 \left[y_2 \ln y_2 \right] \\ s.t. \quad & y_1 + y_2 = 1 \\ & 0 \leq \ y_1, y_2 \ \leq 1 \end{aligned}$$

It is seen that the nonconvexities of the problem lie in the separable concave portion of the objective function. If the trivial solution is tested for stability, Table 10 gives the resulting chemical potentials, while Figure 5 shows the objective function as a nonconvex curve that represents the tangent plane distance function for this case. Note that there is a local maximum of zero at $y_1 \approx 0.5$, but this is the largest value the objective function takes. Thus, it is a relatively easy problem, as any local solver will converge to one of the two local minima that yields a negative tangent plane distance, and so correctly identify that the one phase solution as unstable. This will not be the case in general, where the global solution of the stability problem may be the only stationary point with a negative distance.

If the postulated solution is the global LL solution, which is also given in Table 10, then the tangent plane distance function will be nonnegative everywhere, and this is shown in Figure 5. Again it is a nonconvex curve, and the branch and bound algorithm correctly identifies the global solution in 62 iterations, with the GOP algorithm consuming a total time of 0.35 cpu sec. The global solutions of the stability problem for both these cases are given in Table 10, along with the usual computational results. The iteration at which the tangent plane distance function becomes negative occurs very early, reflecting behavior already seen in the case of the NRTL equation.

Example 5: Ethylene glycol – Lauryl Alcohol – Nitromethane

This example was studied by Null (1970) who used the extended version of the van Laar equation to model the activity coefficients. Chakravarty *et al.* (1985) supplied the coefficients for use in the UNIQUAC equation and these are given in Table 11. The pure component data is supplied in Table 12. Two sets of feed conditions are analyzed:

$$\text{Condition (i):} \quad \{n_i^T\} \equiv \{0.4, 0.3, 0.3\}$$
$$\text{Condition (ii):} \quad \{n_i^T\} \equiv \{0.2, 0.3, 0.5\}$$

There are three potential liquid phases and a vapor phase is not considered. For each feed condition, three postulated solutions obtained from the minimization of the Gibbs free energy are tested, corresponding to the trivial one phase solution, a local LL solution and the global LLL solution. These solutions are supplied in Tables 13 and 14, with their corresponding chemical potential values.

It should be noted that Sun and Seider (1994) report the local LL solution given in Table 14 as the global solution for Condition (ii). The stability analysis yields a tangent plane distance function of $\mathcal{F}^* = -0.027$ for this case, indicating that this postulated solution is not the equilibrium one. When solved locally 100 times, MINOS5.4 had 44 failures in terms of identifying that this local LL solution is not the equilibrium one. The actual global LLL solution has the same mol fractions in each of the three phases as for Condition (i); only the phase fractions change with $\phi^{L_1} = 0.608$ and $\phi^{L_2} = 0.363$. The stability formulation is therefore exactly the same as it was for Condition (i), and is therefore not shown in Table 14.

This example demonstrates the inherent dangers of using local approaches for the phase stability problem. It also again shows that the branch and bound algorithm ascertains instability at a very early iteration. The full results for both sets of feed conditions are given in Tables 13 and 14 and again clearly indicate the greater computational expense required to verify equilibrium solutions.

Example 6: SBA – DSBE – Water

This system involves the modeling of the ARCO SBA-II tower for the dehydration of secbutanol using di-sec-butyl-ether. Kovach and Seider (1987a, 1987b) have performed extensive dynamic analysis of the column itself. There is a temperature gradient in the column that represents the addition of an extra liquid phase. The phase boundaries are very sensitive to all of the parameters used to model the system.

Kovach and Seider (1988) reported vapor-liquid and liquid-liquid equilibrium data for the system SBA–$DSBE$–H_2O. UNIQUAC interaction coefficients were obtained that adequately modeled the VL and LL equilibrium data separately, but not both. Thus, compromise coefficients were found which could accurately represented the data and they are given in Table 15. Widagdo *et al.* (1992) plotted the phase diagrams for 5 trays in the column. They reveal the sensitivity of the lower trays in the column as the phase regions shrink further together. The data for the Antoine equation used to calculate the saturated pressures is supplied by Kovach and Seider (1987b). The temperature, pressure and feed mol fractions for the components are given for these 5 trays in Table 17. The vapor phase is presumed to behave ideally. Two additional sets of conditions studied by Sun and Seider (1994) on tray 28 were also examined, and these are discussed first.

Feed Condition (i) on Tray 28

A comprehensive set of local minima satisfying equality of chemical potentials were used as postulated solutions to test the phase stability algorithm for $\{n_i^T\} \equiv \{0.40, 0.04, 0.56\}$, with the temperature and pressure as for Tray 28. These correspond to the one-phase liquid solution, a local LV solution, a local LL solution and the global LLV solution. The chemical potentials arising from these mol fractions are given in Table 18. As the quality of the solution increases, there is a commensurate rise in the time taken to obtain the global solution to the stability problem. The local LL solution yields a nonnegative tangent plane distance function, which indicates stability with respect to perturbations in the two liquid phases; however, if this solution is tested for stability with respect to the formation of a vapor phase, then a negative tangent plane distance function is obtained, indicating that the postulated solution containing only liquid phases is not the true equilibrium one. Note that the local LV solution was the only one that led to failures when the problem was solved locally.

Feed Condition (ii) on Tray 28

The feed conditions are given as $\{n_i^T\} \equiv \{0.1, 0.1, 0.8\}$. In this case the global solution has one vapor and one liquid phase. Some selected other local postulated solutions (trivial L and local LL) are given in Table 19 with their calculated chemical potentials and computational results. Again, the local LL solution yields a nonnegative tangent plane distance function, but if this solution is tested for the formation of a vapor phase, a negative tangent plane distance is obtained, showing that this solution is unstable with respect to the formation of a vapor phase.

Conditions on all 5 trays

The results for the five trays at the original feed conditions in the column itself are given in Table 20. These were obtained using the trivial one phase liquid solution as the postulated solution. Again, the tangent plane distance becomes negative at an early stage of the algorithm. There were no instances of failure when the problem was solved 100 times locally using MINOS5.4 on any of the trays, but the global solution was not obtained in all cases. A negative tangent plane distance was obtained at the first iteration on all trays, showing how little cpu time is required to verify instability for these five trays. Notice that as one proceeds down the column (tray 2 is at the top of the column), the cpu times and number of iterations increase, indicating that the most difficult trays lie at the lower end of the column.

Table 21 shows the results when the solution corresponding to a global minimum of the Gibbs free energy function is used to generate the tangent plane distance function. The global solutions on all five trays are LLV solutions. The stability test for the ideal vapor phase obviously yields a nonnegative global solution in all cases. Therefore, because the only phase types considered are ideal vapor and liquid phases that can be described by the UNIQUAC equation, this means that it can be definitively asserted that the solutions shown in Table 21 are the equilibrium ones. Note that the fathoming rate remains high.

5 Conclusions

It has been shown how global solutions can be obtained for the phase stability problem, when non-ideal liquid phases are modeled using the NRTL and UNIQUAC equations. In the case of the NRTL equation, a biconvex objective function was minimized over a bilinear set of constraints, and the GOP algorithm (Floudas and Visweswaran, 1990, 1993) was used to obtain global solutions. For the UNIQUAC equation, a number of changes were made in the way the objective function was structured so that it could be recast as the difference of two convex functions, where the concave part was separable. A branch and bound algorithm (Falk and Soland, 1969) was then used to guarantee obtaining global solutions to this problem. The advantage of a global optimization approach is that if the tangent plane distance function of a postulated equilibrium solution can be asserted to be nonnegative, then this solution corresponds to a global minimum of the Gibbs free energy. The computational results also demonstrate the efficiency of the algorithms, noting that the most challenging example takes under half a minute of real time. This is the first approach that can guarantee a postulated solution is a globally stable equilibrium one for this important class of problems. McDonald and Floudas (1994c) show how the same guarantees can be made for other models such as the UNIFAC, ASOG, Wilson, T–K–Wilson for the liquid phase, and the B–truncated virial equation for non–ideal vapor phases.

Acknowledgement: The authors gratefully acknowledge financial support from the National Science Foundation under Grants CBT-8857013 and CTS-9221411, as well as support from Amoco Chemical Co., Exxon Co., Tennessee Eastman Co., Mobil Co., and Shell Development Co.

References

T.F. Anderson and J.M. Prausnitz. Application of the UNIQUAC equation to calculation of multicomponent phase equilibria. 1. vapor-liquid equilibria. *Ind. Eng. Chem. Proc. Des. Dev.*, 17:552, 1978.

L.E. Baker, A.C. Pierce, and K.D. Luks. Gibbs energy analysis of phase equlibria. *Soc. Petro. Eng. J.*, page 731, October 1982.

E. Bender and U. Block. Thermodynamische berechnung der flüssig-flüssig-extraktion. *Verfahrenstechnik*, 9(3):106, 1975.

U. Block and B. Hegner. Development and application of a simulation model for three-phase distillation. *AIChE J.*, 22(3):582, 1976.

J. Castillo and I.E. Grossmann. Computation of phase and chemical equilibria. *Comput. chem. engng.*, 5:99, 1981.

T. Chakravarty, C.W. White, III, and W.D. Seider. Computation of phase equilibrium: optimization with thermodynamic inconsistency. *AIChE J.*, 31(2):316, 1985.

P.T. Eubank, A.E. Elhassen, M.A. Barrufet, and W.B. Whiting. Area method for prediction of fluid-phase equilibria. *I&EC Res.*, 31:942, 1992.

J.E. Falk and R.M. Soland. An algorithm for separable nonconvex programming problems. *Manag. Sci.*, 15(9):550, 1969.

C.A. Floudas and V. Visweswaran. A global optimization algorithm (GOP) for certain classes of nonconvex NLPs: I. Theory. *Comput. chem. engng.*, 14(12):1397, 1990.

C.A. Floudas and V. Visweswaran. A primal-relaxed dual global optimization approach. *Journal of Optimization Theory and Applications*, 78(2):187, 1993.

R. Gautam and W.D. Seider. Computation of phase and chemical equilibrium, Part II: Phase-splitting. *AIChE J.*, 25(6):999, 1979.

J.W. Gibbs. Graphical methods in the thermodynamics of fluids. *Trans. Connecticut Acad.*, 2:311, May 1873a.

J.W. Gibbs. A method of geometrical representation of the thermodynamic properties of substances by means of surfaces. *Trans. Connecticut Acad.*, 2:382, May 1873b.

A.K. Gupta, P.R. Bishnoi, and N. Kalogerakis. A method for the simultaneous phase equilibria and stability calculations for multiphase reacting and non-reacting systems. *Fluid Phase Equilibria*, 63:65, 1991.

R.A. Heidemann and J.M. Mandhane. Some properties of the NRTL equation in correcting liquid-liquid equilibrium data. *Chem. Eng. Sci.*, 28:1213, 1973.

R. Horst and H. Tuy. *Global Optimization.* Springer-Verlag, 1st. edition, 1990.

J.W. Kovach and W.D. Seider. Heterogeneous azeotropic distillation: experimental and simulation results. *AIChE J.*, 33(8):1300, 1987a.

J.W. Kovach and W.D. Seider. Heterogeneous azeotropic distillation – homotopy-continuation methods. *Comput. chem. engng.*, 11(6):593, 1987b.

J.W. Kovach and W.D. Seider. Vapor-liquid and liquid-liquid equilibrium for the system sec-butyl-alcohol – di- sec-butyl ether – water. *J. Chem. Eng. Data*, 33:16, 1988.

G. Lantagne, B. Marcos, and B. Cayrol. Computation of complex equilibria by nonlinear optimization. *Comput. chem. engng.*, 12(6):589, 1988.

C.M. McDonald and C.A. Floudas. Global optimization for the phase and chemical equilibrium problem: application to the NRTL equation. accepted by *Comput. chem. engng.*. 1994a.

C.M. McDonald and C.A. Floudas. Decomposition based and branch and bound global optimization approaches for the phase equilibrium problem. *Journal of Global Optimization*, in press. 1994b.

C.M. McDonald and C.A. Floudas. GLOPEQ: A new computational tool for the phase and chemical equilibrium problem. in preparation. 1994c.

M.L. Michelsen. The isothermal flash problem - Part I. Stability. *Fluid Phase Equilibria*, 9:1, 1982a.

M.L. Michelsen. The isothermal flash problem - Part II. Phase-split calculation. *Fluid Phase Equilibria*, 9:21, 1982b.

N.R. Nagarajan, A.S. Cullick, and A. Griewank. New strategy for phase equilibrium and critical point calculations by thermodynamic energy analysis. Part I. Stability analysis and flash. *Fluid Phase Equilibria*, 62:191, 1991a.

N.R. Nagarajan, A.S. Cullick, and A. Griewank. New strategy for phase equilibrium and critical point calculations by thermodynamic energy analysis. Part II. Critical Point Calculations. *Fluid Phase Equilibria*, 62:211, 1991b.

H.R. Null. *Phase equilibrium in process design.* Wiley-Interscience, New York, 1970.

G.E. Paules, IV and C.A. Floudas. A new optimization approach for phase and chemical equilibrium problems. Paper presented at the Annual AIChE Meeting, San Franciso, CA, November, 1989.

H. Renon and J.M. Prausnitz. Local compositions in thermodynamic excess functions for liquid mixtures. *AIChE J.*, 14(1):135, 1968.

J.V. Smith, R.W. Missen, and W.R. Smith. General optimality criteria for multiphase multireaction chemical equilibrium. *AIChE J.*, 39(4):707, 1993.

A.C. Sun and W.D. Seider. Homotopy-continuation for stability analysis in the global minimization of the Gibbs free energy. *Fluid Phase Equilibria*, 1994. In Press.

D.J. Swank and J.C. Mullins. Evaluation of methods for calculating liquid-liquid phase-splitting. *Fluid Phase Equilibria*, 30:101, 1986.

F.F.Y. Walraven and P.V. van Rompay. An improved phase-splitting algorithm. *Comput. chem. engng.*, 12(8):777, 1988.

S. Widagdo, W.D. Seider, and D.H. Sebastian. Dynamic analysis of heterogeneous azeotropic distillation. *AIChE J.*, 38(8):1229, 1992.

Appendix A

In what follows, k_S represents any node of the solution tree, with k_t representing a temporarily assigned node used in the selection of previous Lagrange functions. $\mathcal{S}_C$ represents the current node under consideration at any given iteration and is obviously a leaf node. The parent of any of these nodes is simply indicated by $p\,(k_S)$. The $\mathcal{X}$ variable bound sets for some B_l are denoted $\hat{\mathcal{X}}^{B_l^K}$ for the current iteration K, and $\hat{\mathcal{X}}^{B_l^{\bar{K}}}$ for previous iterations $\bar{K} \in PL(\bar{K})$. The set I_{k_S} represents the iteration number K, at which a particular node k_S is generated. The complete algorithm for the NRTL equilibrium model is now given.

STEP 0: Initialization

Initialize $K = 0$, $\mathcal{L}^R_{y_i} = 0$,$\mathcal{U}^R_{y_i} = 1 \; \forall \; i$, $P^U = +\infty$, $M^L = -\infty$, $\mathcal{S}_C = R$, $k_S = \emptyset$. Select y^0 and ε.

STEP 1: Primal Problem

Evaluate $\mathcal{F}(y^K)$ and store λ^K , y^K. If $\mathcal{F}(y^K) < P^U$, solve (S-N) locally to give $\mathcal{F}^*$.
Update $P^U = \min\,[P^U, \mathcal{F}(y^K), \mathcal{F}^*]$.

STEP 2: Select previous Lagrangians

Set $PL(\bar{K}) = \emptyset$, $k_t = \mathcal{S}_C$.
while ($k_t \neq R$)
do $\bar{K} = I_{k_t}$, $PL(\bar{K}) = PL(\bar{K}) \cup \bar{K}$, $k_t = p\,(k_t)$.

STEP 3: The Relaxed Dual Phase

(1) Choose a combination of qualifying constraints, B_l, from the set CB.
Use $s_i^{B_l}$ and $R_K\{\mathcal{L}^R,\mathcal{U}^R\}$ to calculate $B\{\mathcal{L}^B,\mathcal{U}^B\}$, and hence $\{\mathcal{L}_{\Psi_i},\mathcal{U}_{\Psi_i}\}$.
Set $\hat{\mathcal{X}}^{B_l^K}$ and $\hat{\mathcal{X}}^{B_l^{\bar{K}}}$ and solve (RD) to give μ_B^* and y^*.

$$
\begin{aligned}
\min_{\substack{y \in Y \\ \mu_B}} \quad & \mu_B \\
s.t. \quad & \mu_B \geq L(\hat{\mathcal{X}}^{B_l^K}, y^K, y, \lambda^K_{\mathcal{X}}) \\
& \mu_B \geq L_{\bar{K}}(\hat{\mathcal{X}}^{B_l^{\bar{K}}}, y^{\bar{K}}, y, \lambda^{\bar{K}}_{\mathcal{X}}) \quad \forall \quad \bar{K} \in PL(\bar{K}) \\
& \mathcal{L}^B_{y_i} \leq \; y_i \; \leq \; \mathcal{U}^B_{y_i} \quad \forall \;\; i \in C
\end{aligned}
$$

$$\sum_{i \in C} y_i = 1$$

(i) If $\mu_B^* \geq P^U - \epsilon$, then fathom solution.

(ii) If $\mu_B^* < P^U - \epsilon$, then set $k_S = k_S + 1$, $p(k_S) = \mathcal{S}_C$, $I_{k_S} = K$, $\mu^{k_S} = \mu_B^*$, $y^{k_S} = y^*$, $R_{k_S}\{\mathcal{L}^R, \mathcal{U}^R\} = B\{\mathcal{L}^B, \mathcal{U}^B\}$.

(2) Choose another set of bounds B_l from CB and return to (1).

If there are no remaining unchosen B_l in CB, then proceed to Step 4.

STEP 4: Select mol vector for next iteration

Select infimum of all $\mu_B^{k_S}$, and set $\mathcal{S}_C = k_S$, the associated node.

Set $y^{K+1} = y^{S_C}$, $M^L = \mu_B^{S_C}$, $R_{K+1}\{\mathcal{L}^R, \mathcal{U}^R\} = R_{S_C}\{\mathcal{L}^R, \mathcal{U}^R\}$.

STEP 5: Check for convergence

Check if $|P^U - M^L| \leq \epsilon$. If true, then STOP; otherwise set $K = K + 1$, and return to Step 1.

It has been shown how all the conditions required to guarantee ϵ-global convergence of the GOP algorithm are satisfied (Floudas and Visweswaran, 1990, 1993).

Appendix B

The complete branch and bound algorithm for the minimization of the tangent plane distance function when the liquid phase is modeled using the UNIQUAC equilibrium model is now given.

STEP 0: Initialization

Select an initial mol vector $y^1 = 0$ and convergence tolerance ε.

Initialize $\mathcal{L}_{y_i}^R = 0$,$\mathcal{U}_{y_i}^R = 1$, $P^U = +\infty$, $M^L = -\infty$, $\mathcal{S}_C = R$, $k_S = \emptyset$, $\{\mathcal{H}_i\} = 0$, $N_P = 0$.

STEP 1: Primal Problem

Evaluate $\mathcal{F}(y^K)$. If $\mathcal{F}(y^K) < P^U$, solve (S-U) locally to give $\mathcal{F}^*$.

Update $P^U = \min\,[P^U, \mathcal{F}(y^K), \mathcal{F}^*]$.

STEP 2: Convex underestimation phase

(1) Choose a combination of box bounds, B_l, from the set CB.

Use $s_i^{B_l}$, $\mathcal{H}_i$ and $R_K\{\mathcal{L}^R,\mathcal{U}^R\}$ to calculate $B\{\mathcal{L}^B,\mathcal{U}^B\}$.

Construct $\Psi_i(y_i)$ based on $B\{\mathcal{L}^B,\mathcal{U}^B\}$ and solve (UES) to give μ^* and y^*.

(i) If $\mu^* \geq P^U - \epsilon$, then fathom solution.

(ii) If $\mu^* < P^U - \epsilon$, then set $k_S = k_S + 1$, $p\,(k_S) = \mathcal{S}_C$, $\mu^{k_S} = \mu^*$, $y^{k_S} = y^*$, $R_{k_S}\{\mathcal{L}^R,\mathcal{U}^R\} = B\{\mathcal{L}^B,\mathcal{U}^B\}$.

(2) Choose another set of bounds B_l from CB and return to (1).

If there are no remaining unchosen B_l in CB, then proceed to Step 3.

STEP 3: Select mol vector for next iteration

Select infimum of all $\mu_B^{k_S}$, and set $\mathcal{S}_C = k_S$, the associated node.

Set $y^{K+1} = y^{S_C}$, $M^L = \mu_B^{S_C}$, $R_{K+1}\{\mathcal{L}^R,\mathcal{U}^R\} = R_{S_C}\{\mathcal{L}^R,\mathcal{U}^R\}$.

Choose $1 \leq N_P \leq N_{CV}$. Set $D = \{i\} \equiv C$, $\{\mathcal{H}_i\} = 0$.

for $m = 1, \ldots, N_P$

$$\begin{aligned} \{i^*\} &= \underset{D}{\text{argmax}}\, |-y_i \ln y_i - \Psi_i(y_i)| \\ \mathcal{H}_{i^*} &= 1 \\ D &= D \backslash \{i^*\} \end{aligned}$$

end

STEP 4: Check for convergence

Check if $|P^U - M^L| \leq \epsilon$. If true, then STOP; otherwise set $K = K + 1$, and return to Step 1.

Convergence to an ϵ-global solution of (DC) by the above algorithm has been proven by Horst and Tuy (1990).

Nature of SP/IP	y_1
Global Minimum	0.0042
Local Minimum	0.500
Local Maximum	0.160
Inflection Point	0.025
Inflection Point	0.279
Inflection Point	0.706
Inflection Point	0.895

Table 1: Stationary points for Example 1

Solutions for n-Butyl-Acetate (1) – Water (2) at T, $P = 1$ atm							
Component	Feed (mols)	$\mu_i^0(z)$ (—)	y^* (—)	$\mathcal{F}^*$ (—)	cpu (sec)	N_I (—)	N_F (%)
$C_6H_{12}O_2$ (1)	0.50	-0.06391	0.00421	-0.03247	0.06	12	33
H_2O (2)	0.50	0.02875	0.99579	(71/29)	(0.02)	(4)	
$C_6H_{12}O_2$ (1)	0.10	0.18825	0.96345	-0.21419	0.07	14	50
H_2O (2)	0.90	0.02412	0.03655	(0/5)	(0.001)	(1)	
$C_6H_{12}O_2$ (1)	0.20	-0.10252	0.00380	-0.07427	0.05	9	28
H_2O (2)	0.80	0.07088	0.99620	(0/100)	(0.01)	(1)	
$C_6H_{12}O_2$ (1)	0.65	-0.02708	0.94131	-0.00671	0.11	22	48
H_2O (2)	0.35	-0.01910	0.05869	(87/13)	(0.001)	(4)	

Table 2: Data and solutions for Example 1 with one liquid phase postulated

Solutions for n-Butyl-Acetate (1) – Water (2) for all feed conditions									
Comp.	Solution	$z_i^{L_1}$ (—)	$z_i^{L_2}$ (—)	$\mu_i^0(z)$ (—)	y^* (—)	$\mathcal{F}^*$ (—)	cpu (sec)	N_I (—)	N_F (%)
$i = 1$	Local LL	0.93514	0.00456	-0.03523	0.59425	-0.00070	0.15	32	45
$i = 2$	$\phi^{L_1} = 0.21001$	0.06486	0.99544	-0.00398	0.40575	(25/75)	(0.002)	(1)	
$i = 1$	Global LL	0.59199	0.00456	-0.03642	0.59199	0.0	0.16	36	43
$i = 2$	$\phi^{L_1} = 0.33271$	0.40801	0.99544	-0.00398	0.40801	(–)	(–)	(–)	

Table 3: Data and global solutions for Example 1

Toluene (1) – Water (2) – Aniline (3)					
Components ij	i	j	τ_{ij}	τ_{ji}	$\alpha_{ij} = \alpha_{ji}$
$C_7H_8 - H_2O$	1	2	4.93035	7.77063	0.2485
$C_7H_8 - C_6H_7N$	1	3	1.59806	0.03509	0.3000
$H_2O - C_6H_7N$	2	3	4.18462	1.27932	0.3412

Table 4: Binary data for Example 2

Solutions for Toluene (1) – Water (2) – Aniline (3) at T, $P = 1$ atm										
Comp.	Solution	$z_i^{L_1}$ (—)	$z_i^{L_2}$ (—)	$\mu_i^0(z)$ (—)	y_i^* (—)	$\mathcal{F}^*$ (—)	cpu (sec)	N_I (—)	N_F (%)
$i = 1$	Trivial L	0.29989	(—)	-0.28809	0.00007	-0.29454	0.18	16	68
$i = 2$	$\phi^{L_1} = 1.0$	0.20006	(—)	0.29158	0.99686	(31/69)	(0.002)	(1)	
$i = 3$		0.50005	(—)	-0.59336	0.00307				
$i = 1$	Global LL	0.34674	0.00009	-0.38371	0.00009	0.0	0.94	85	66
$i = 2$	$\phi^{L_1} = .865$	0.07584	0.99495	-0.00461	0.99495	(–)	(–)	(–)	
$i = 3$		0.57742	0.00496	-0.47388	0.00496				

Table 5: Data and global solutions for Example 2

n-Propanol (1) – n-Butanol (2) – Water (3): τ_{ij} and α_{ij} dimensionless					
Components ij	i	j	τ_{ij}	τ_{ji}	$\alpha_{ij} = \alpha_{ji}$
C_3H_8O – $C_4H_{10}O$	1	2	-0.61259	0.71640	0.30
C_3H_8O – H_2O	1	3	-0.07149	2.7425	0.30
$C_4H_{10}O$ – H_2O	2	3	0.90047	3.51307	0.48

Table 6: Binary data for Example 3

Solutions for n-Propanol (1) – n-Butanol (2) – Water (3) at T, $P = 1$ atm									
Comp.	Solution	$z_i^{L_1}$ (—)	$z_i^{L_2}$ (—)	$\mu_i^0(z)$ (—)	y_i^* (—)	$\mathcal{F}^*$ (—)	cpu (sec)	N_I (—)	N_F (%)
$i = 1$	Trivial L	0.16	(—)	-0.71239	0.01905	-0.01161	0.62	53	67
$i = 2$	$\phi^{L_1} = 1.0$	0.80	(—)	-0.00681	0.97154	(0/31)	(0.002)	(1)	
$i = 3$		0.04	(—)	-2.56507	0.00941				
$i = 1$	Global LL	0.26390	0.02214	-0.69700	0.02214	0.0	2.37	213	64
$i = 2$	$\phi^{L_1} = .570$	0.67456	0.96645	-0.02023	0.96645	(–)	(–)	(–)	
$i = 3$		0.06154	0.01141	-2.46114	0.01141				

Table 7: Data and global solutions for Example 3, Conditions (i)

Solutions for n-Propanol (1) – n-Butanol (2) – Water (3) near plait point									
Comp.	Solution	$z_i^{L_1}$ (—)	$z_i^{L_2}$ (—)	$\mu_i^0(z)$ (—)	y_i^* (—)	$\mathcal{F}^*$ (—)	cpu (sec)	N_I (—)	N_F (%)
$i = 1$	Trivial L	0.052	(—)	-1.80016	0.03599	-9.85×10^{-6}	4.98	549	57
$i = 2$	$\phi^{L_1} = 1.0$	0.800	(—)	-0.04875	0.84967	(60/40)	(0.02)	(1)	
$i = 3$		0.148	(—)	-0.93380	0.11434				
$i = 1$	Global LL	0.05509	0.03707	-1.80055	0.03707	0.0	7.09	757	51
$i = 2$	$\phi^{L_1} = .828$	0.79043	0.84620	-0.04880	0.84620	(–)	(–)	(–)	
$i = 3$		0.15447	0.11673	-0.93341	0.11673				

Table 8: Global solutions for Example 3, Conditions (ii)

Toluene (1) – Water (2)		
Parameter	$i=1$	$i=2$
q_i	2.97	1.40
q_i'	2.97	1.00
r_i	3.92	0.92
l_i	1.83	-2.32
z_i^R	3.53316	6.52174
z_i^B	2.98858	0
φ_i	28.53522	7.0

Table 9: Pure component data for Example 4

Solutions for Toluene (1) – Water (2) at $T = 295$K, $P = 1$ atm									
Comp.	Solution	$z_i^{L_1}$ (—)	$z_i^{L_2}$ (—)	$\mu_i^0(z)$ (—)	y^* (—)	$\mathcal{F}^*$ (—)	cpu (sec)	N_I (—)	N_F (%)
$i=1$	Trivial L	0.5	(—)	0.00007	0.00049	-0.61887	0.19	39	42
$i=2$	$\phi^{L_1} = 1.0$	0.5	(—)	0.61839	0.99951	(0/68)	(0.04)	(1)	
$i=1$	Global LL	0.95642	0.00089	-0.03864	0.95642	0.0	0.30	62	38
$i=2$	$\phi^{L_1} = .478$	0.04358	0.99911	-0.00088	0.04358	(–)	(–)	(–)	

Table 10: Global solutions for Example 4

Ethylene Glycol (1) – Lauryl Alcohol (2) – Nitromethane (3) $\tau_{ij} = \exp(-\Delta u_{ij}/RT)$ with T in K				
Components ij	i	j	$\Delta u_{ij}/R$	$\Delta u_{ji}/R$
$C_2H_6O_2 - C_{12}H_{26}O$	1	2	247.20	69.69
$C_2H_6O_2 - CH_3NO_2$	1	3	54.701	467.88
$C_{12}H_{26}O - CH_3NO_2$	2	3	305.52	133.19

Table 11: Binary data for Example 5

$C_2H_6O_2$ (1) – $C_{12}H_{26}O$ (2) – CH_3NO_2 (3)			
Parameter	$i = 1$	$i = 2$	$i = 3$
$q_i = q_i'$	2.2480	7.3720	1.8680
r_i	2.4088	8.8495	2.0086
l_i	-0.6048	-0.4620	-0.3056

Table 12: Pure component data for Example 5

Solutions for Ethylene Glycol (1) – Lauryl Alcohol (2) – Nitromethane (3) at $T = 295$K, $P = 1$ atm										
Comp.	Solution	$z_i^{L_1}$ (—)	$z_i^{L_2}$ (—)	$z_i^{L_3}$ (—)	$\mu_i^0(z)$ (—)	y_i^* (—)	$\mathcal{F}^*$ (—)	cpu (sec)	N_I (—)	N_F (%)
$i=1$	Trivial L	0.4	(—)	(—)	-0.09120	0.75425	-0.11395	10.70	753	70
$i=2$	$\phi^{L_1} = 1.0$	0.3	(—)	(—)	-0.66963	0.00222	(10/86)	(0.07)	(1)	
$i=3$		0.3	(—)	(—)	0.00187	0.24353				
$i=1$	Local LL	.27078	.61986	(—)	-0.27095	0.02334	-0.05877	10.97	788	70
$i=2$	$\phi^{L_1} = .630$	.47302	.00562	(—)	-0.55375	0.00173	(72/28)	(1.17)	(4)	
$i=3$		.25620	.37452	(—)	0.03965	0.97493				
$i=1$	Global LLL	.27899	.02776	.69280	-0.23994	0.27899	0.0	29.70	2144	69
$i=2$	$\phi^{L_1} = 0.608$	.49191	.00206	.00399	-0.54068	0.49191	(–)	(–)	(–)	
$i=3$	$\phi^{L_2} = 0.029$	.22910	.97018	.30321	-0.02161	0.22910				

Table 13: Data and solutions for Example 5, Conditions (i)

Solutions for Ethylene Glycol (1) – Lauryl Alcohol (2) – Nitromethane (3) at $T = 295$K, $P = 1$ atm									
Comp.	Solution	$z_i^{L_1}$ (—)	$z_i^{L_2}$ (—)	$\mu_i^0(z)$ (—)	y_i^* (—)	$\mathcal{F}^*$ (—)	cpu (sec)	N_I (—)	N_F (%)
$i=1$	Trivial L	0.2	(—)	-0.50936	0.01254	-0.22827	7.31	544	68
$i=2$	$\phi^{L_1} = 1.0$	0.3	(—)	-0.54294	0.00113	(0/77)	(0.07)	(1)	
$i=3$		0.5	(—)	0.21650	0.98633				
$i=1$	Local LL	0.29672	0.03001	-0.20102	0.71540	-0.02700	13.43	957	70
$i=2$	$\phi^{L_1} = .637$	0.46950	0.00211	-0.56343	0.00336	(44/56)	(0.21)	(2)	
$i=3$		0.23378	0.96788	-0.02272	0.28124				

Table 14: Solutions for Example 5, Conditions (ii)

SBA (1) – DSBE (2) – Water (3)				
$\tau_{ij} = \exp\left(-\Delta u_{ij}/RT\right)$ with T in K , $R = 1.9872$				
Components ij	i	j	Δu_{ij}	Δu_{ji}
C_3H_8O – $C_4H_{10}O$	1	2	-193.140	415.850
C_3H_8O – H_2O	1	3	424.025	103.810
$C_4H_{10}O$ – H_2O	2	3	315.312	3922.500

Table 15: Binary data for Example 6

SBA (1) – DSBE (2) – Water (3)			
Parameter	$i = 1$	$i = 2$	$i = 3$
q_i	3.6640	5.1680	1.4000
q_i'	4.0643	5.7409	1.6741
r_i	3.9235	6.0909	0.9200

Table 16: Pure component data for Example 6

SBA (1) – DSBE (2) – Water (3)		
Tray (—)	Temperature (K)	Pressure (atm)
28	363.20	1.170
25	362.35	1.166
7	361.67	1.145
5	361.58	1.143
2	361.50	1.140

Table 17: Temperatures and Pressures for Example 6

Solutions for SBA (1) – DSBE (2) – Water (3) on Tray 28											
Comp.	Solution	$z_i^{L_1}$ (—)	$z_i^{L_2}$ (—)	z_i^{V} (—)	$\mu_i^0(z)$ (—)	y_i^* (—)	$\mathcal{F}^*$ (—)	cpu (sec)	N_I (—)	N_F (%)
$i=1$	Trivial L	0.40	(—)	(—)	-1.05176	.03446	-0.07354	5.66	390	70
$i=2$	$\phi^{L_1}=1.0$	0.04	(—)	(—)	-1.83427	0.0	(0/31)	(0.08)	(1)	
$i=3$		0.56	(—)	(—)	-0.31851	.96554				
$i=1$	Local LV	.43309	(—)	.33352	-0.94108	.04907	-0.02858	7.57	532	69
$i=2$	$\phi^{L_1}=.668$	.02200	(—)	.07616	-2.41798	0.0	(71/29)	(0.23)	(2)	
$i=3$		.54491	(—)	.59032	-0.37012	.95093				
$i=1$	Local LL	.51963	.05616	(—)	-0.92395	.51963	0.0	17.63	1299	68
$i=2$	$\phi^{L_1}=.742$	.05392	0.0	(—)	-2.25146	.05392	(–)	(–)	(–)	
$i=3$		.42645	.94384	(—)	-0.40123	.42645				
$i=1$	Global LLV	.51802	.05667	.34024	-0.92115	.51802	0.0	17.87	1306	67
$i=2$	$\phi^{L_1}=0.723$	.05110	0.0	.08762	-2.27779	.05110	(–)	(–)	(–)	
$i=3$	$\phi^{L_2}=0.242$	.43088	.94333	.57214	-0.40139	.43088				

Table 18: Data and solutions for Example 6, Conditions (i) on Tray 28

Solutions for SBA (1) – DSBE (2) – Water (3) on tray 28									
Comp.	Solution	$z_i^{L_1}$ (—)	$z_i^{L_2}/z_i^V$ (—)	$\mu_i^0(z)$ (—)	y_i^* (—)	$\mathcal{F}^*$ (—)	cpu (sec)	N_I (—)	N_F (%)
$i=1$	Trivial L	0.10	(—)	−2.95686	.00554	−1.57107	3.90	273	68
$i=2$	$\phi^{L_1}=1.0$	0.10	(—)	0.55366	.96516	(0/81)	(0.08)	(1)	
$i=3$		0.80	(—)	−0.00551	.02930				
$i=1$	Local LL	.35241	.02801	−1.23873	.35241	0.0	13.83	1020	70
$i=2$	$\phi^{L_1}=.222$	.45059	0.0	−1.42186	.45059	(–)	(–)	(–)	
$i=3$		.19700	.97199	−0.38841	.19700				
$i=1$	Global LV	.01955	.19682	−1.46848	.01956	0.0	5.06	352	71
$i=2$	$\phi^{L_1}=.546$	0.0	.22036	−1.35554	0.0	(–)	(–)	(–)	
$i=3$		.98045	.58282	−0.38291	.98044				

Table 19: Data and solutions for Example 6, Conditions (ii) on Tray 28

Solutions for SBA (1) – DSBE (2) – Water (3) on five trays								
Comp.	Tray	$z_i = n_i^T$ (—)	$\mu_i^0(z)$ (—)	y_i^* (—)	$\mathcal{F}^*$ (—)	cpu (sec)	N_I (—)	N_F (%)
$i=1$	28	0.40307	−1.08878	0.03110	−0.09081	5.36	362	71
$i=2$		0.05150	−1.73926	0.0	(0/31)	(0.08)	(1)	
$i=3$		0.54543	−0.29940	0.96890				
$i=1$	25	0.35184	−1.41935	0.01571	−0.23644	3.20	219	70
$i=2$		0.12553	−1.38417	0.0	(0/35)	(0.08)	(1)	
$i=3$		0.52263	−0.17587	0.98429				
$i=1$	7	0.33452	−1.55739	0.01227	−0.31322	2.87	190	70
$i=2$		0.18212	−1.41597	0.0	(0/47)	(0.08)	(1)	
$i=3$		0.48336	−0.12255	0.98773				
$i=1$	5	0.31392	−1.64307	0.01049	−0.35782	2.63	180	71
$i=2$		0.20360	−1.39570	0.0	(0/62)	(0.08)	(1)	
$i=3$		0.48248	−0.07983	0.98951				
$i=1$	2	0.31286	−1.65110	0.01035	−0.36364	2.59	178	70
$i=2$		0.21005	−1.40490	0.0	(0/62)	(0.08)	(1)	
$i=3$		0.47709	−0.07707	0.98965				

Table 20: Feed data and solutions for Example 6 (one liquid phase postulated)

Solutions for SBA (1) – DSBE (2) – Water (3) on five trays								
Comp.	Solution	$z_i^{L_1}$ (—)	$z_i^{L_2}$ (—)	z_i^V (—)	$\mu_i^0(z)$ (—)	cpu (sec)	N_I (—)	N_F (%)
$i=1$	Tray 28	0.51802	0.05667	0.34024	-0.92114	19.67	1306	67
$i=2$	$\phi^{L_1}=0.607$	0.05110	0.0	0.08762	-2.27779			
$i=3$	$\phi^{L_2}=0.159$	0.43088	0.94333	0.57214	-0.40139			
$i=1$	Tray 25	0.52037	0.04401	0.30236	-1.04217	16.41	1172	69
$i=2$	$\phi^{L_1}=0.394$	0.15429	0.0	0.13931	-1.81712			
$i=3$	$\phi^{L_2}=0.141$	0.32534	0.95599	0.55833	-0.42883			
$i=1$	Tray 7	0.48182	0.03759	0.28014	-1.13669	15.26	1082	70
$i=2$	$\phi^{L_1}=0.345$	0.24579	0.0	0.16430	-1.67032			
$i=3$	$\phi^{L_2}=0.062$	0.27239	0.96241	0.55556	-0.45201			
$i=1$	Tray 5	0.45250	0.03474	0.26923	-1.17847	14.48	1050	70
$i=2$	$\phi^{L_1}=0.365$	0.29858	0.0	0.17512	-1.60852			
$i=3$	$\phi^{L_2}=0.095$	0.24892	0.96526	0.55565	-0.45390			
$i=1$	Tray 2	0.44619	0.03419	0.26708	-1.18954	15.16	1065	70
$i=2$	$\phi^{L_1}=0.464$	0.30924	0.0	0.17717	-1.60002			
$i=3$	$\phi^{L_2}=0.160$	0.24457	0.96581	0.55575	-0.45678			

Table 21: Solutions for Example 6, global solution postulated

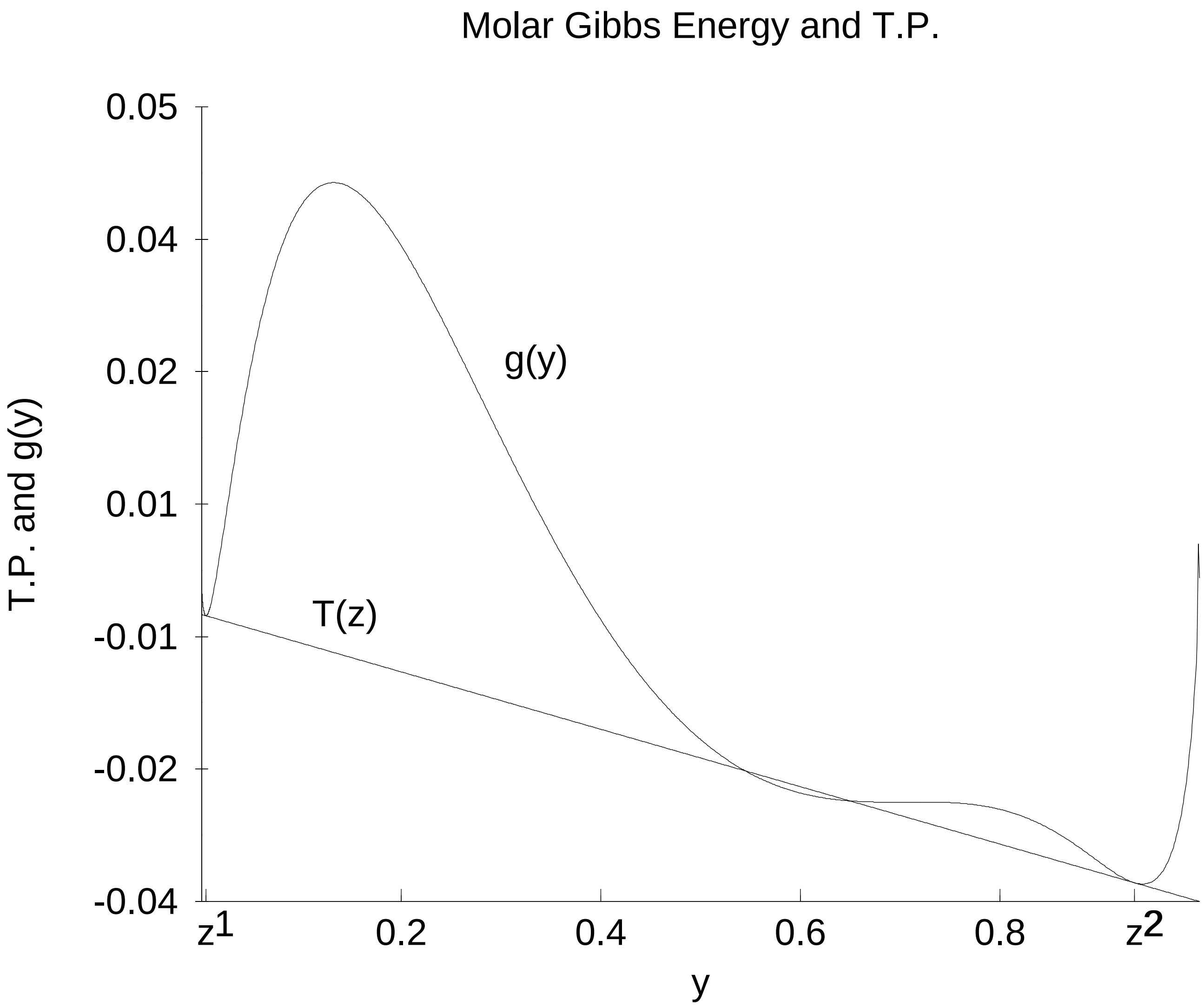

Figure 1: Illustration of stability for non-equilibrium case

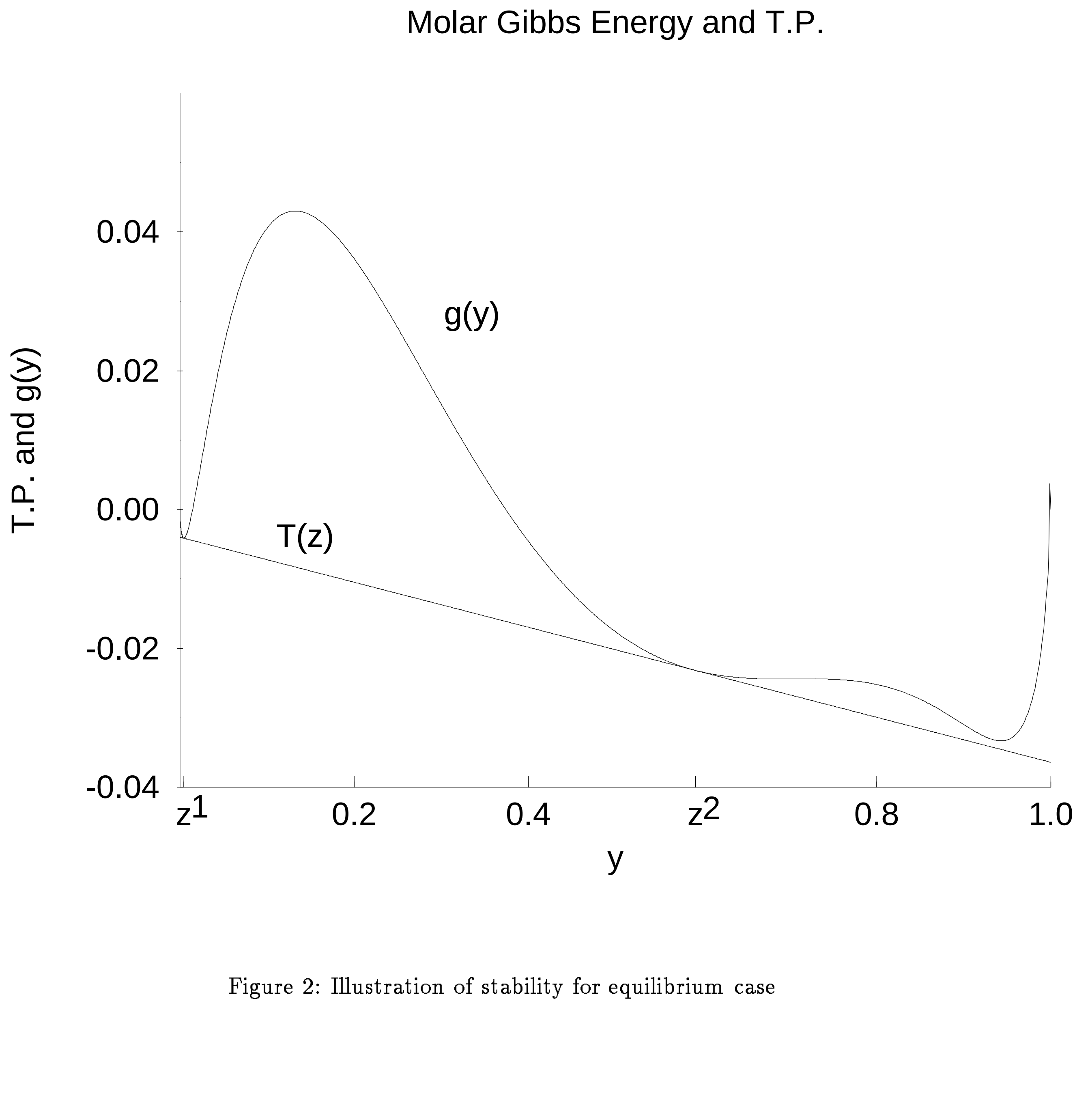

Figure 2: Illustration of stability for equilibrium case

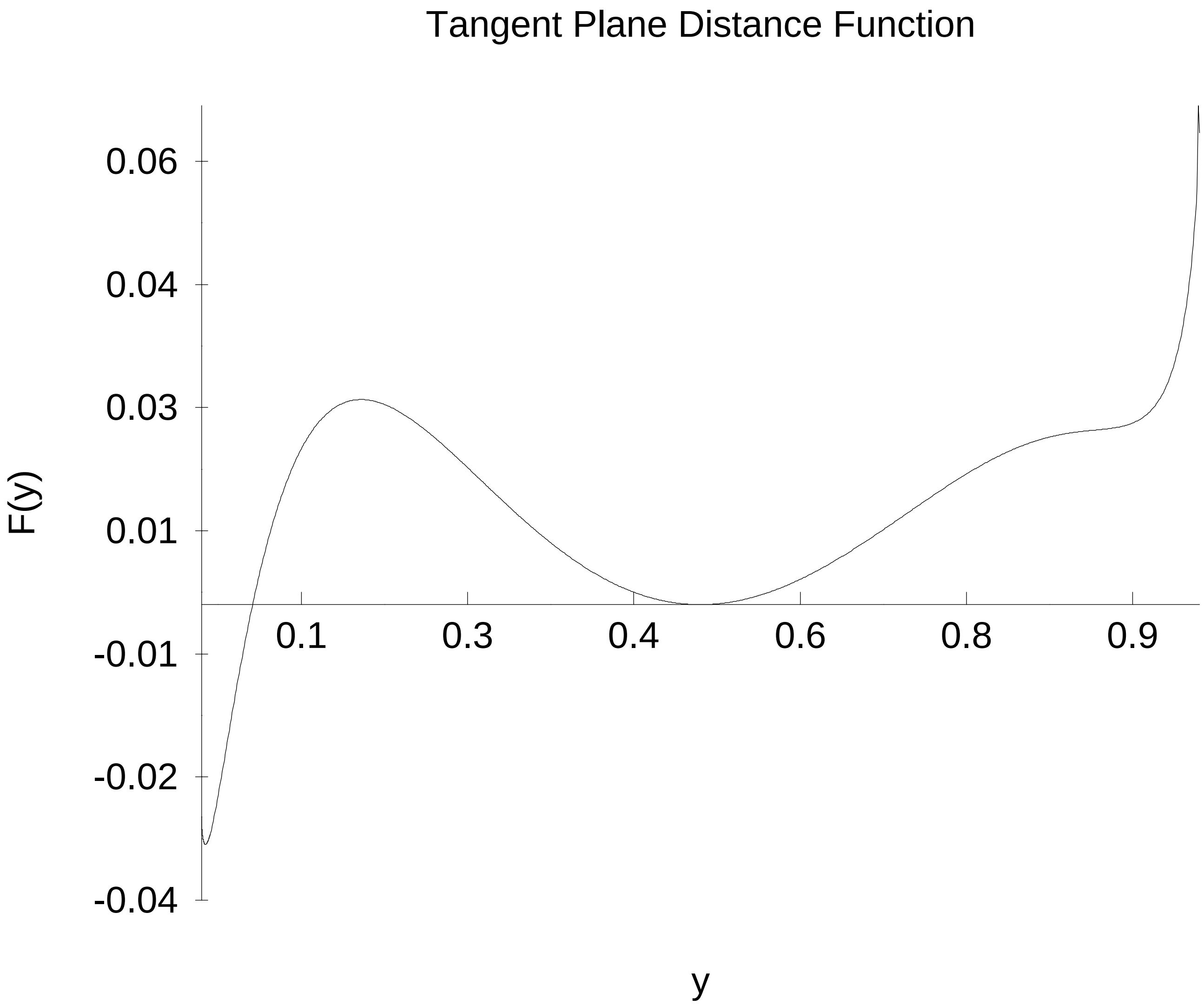

Figure 3: Plot of $\mathcal{F}(y_1)$ for Example 1

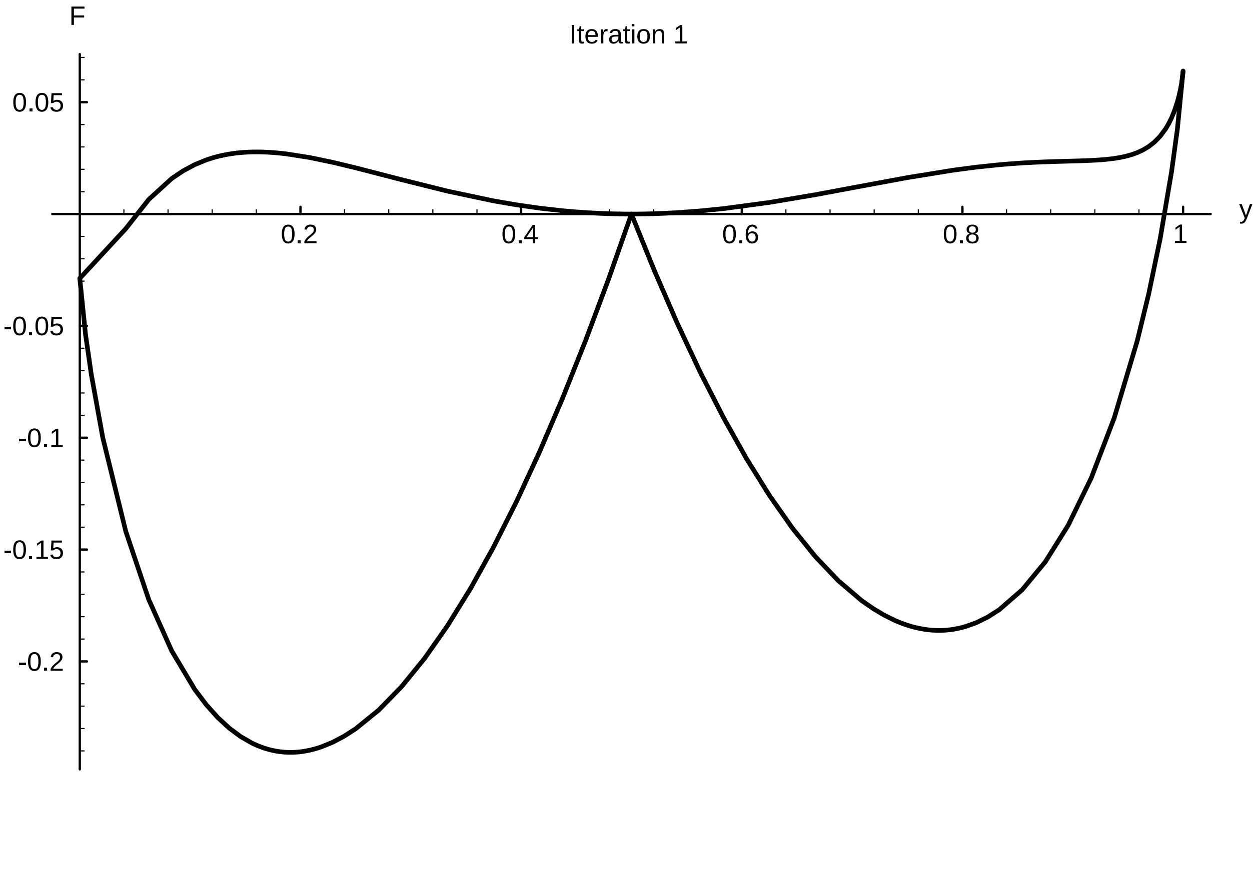

Figure 4: Plot of $\mathcal{F}(y)$ and underestimating Lagrangians for Iteration 1

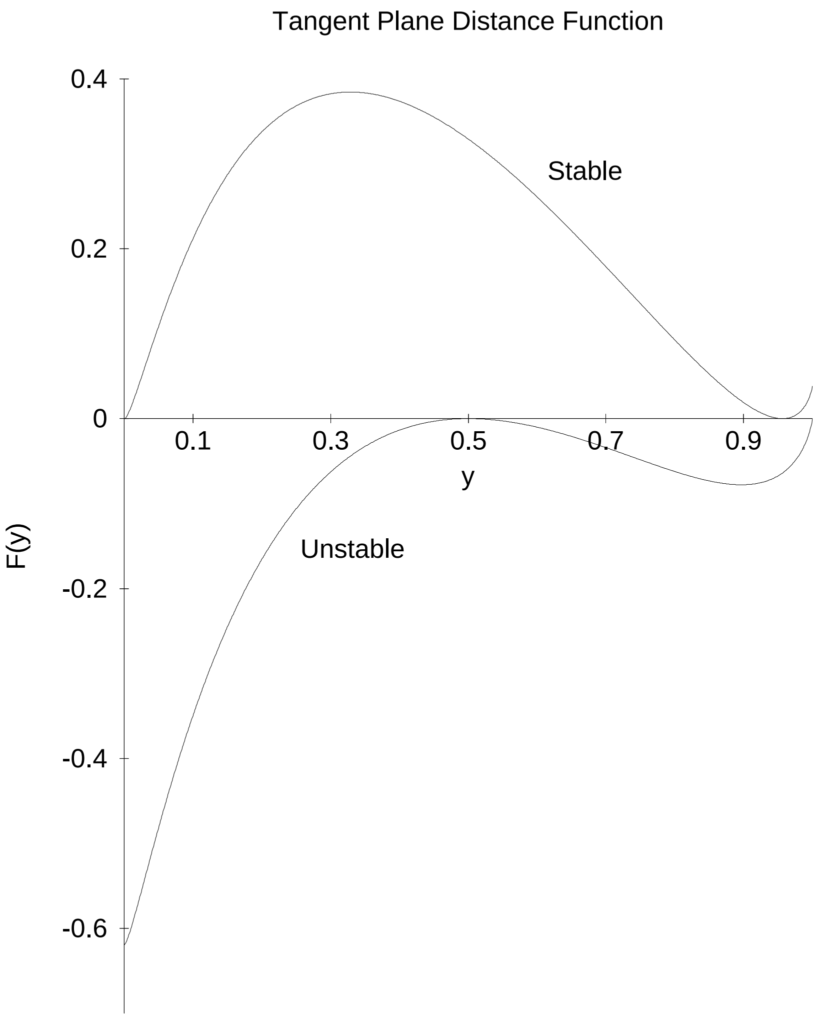

Figure 5: Plot of $\mathcal{F}(y)$ for Example 4, trivial and global solutions postulated